# ABSTRACT


| | |
|---|---|
| Title of Thesis: | EVALUATING CARBON SEQUESTRATION POTENTIAL OF NATURAL AND RESTORED TIDAL MARSHES IN CHESAPEAKE BAY THROUGH QUANTIFICATION OF METHANE FLUXES AND IDENTIFICATION OF DRIVERS |
| | Daniella Marie Hanacek, Master of Science, 2022 |
| Thesis directed by: | Doctor Lorie Staver and Doctor Jeffrey Cornwell, University of Maryland Center For Environmental Science, Horn Point Laboratory |



The production of methane in brackish marshes may offset the carbon sequestered by these wetlands. Brackish tidal marshes are widespread in Chesapeake Bay and there exists a need for understanding the carbon balance of these ecosystems. This thesis presents the results of measurements of methane flux, through static flux chamber experiments, and analysis of marsh porewater to examine biogeochemical and plant-mediated drivers of methane flux in marshes of Chesapeake Bay. In addition, there is growing interest from the scientific and resource management community in how natural marshes cycle carbon and whether restored marshes show biogeochemical similarities. Therefore, I tested my hypotheses in the natural marshes of Monie Bay, part of the Chesapeake Bay National Estuarine Research Reserve – Maryland, and in restored tidal marshes created with dredged sediments at Poplar Island. Methane emissions offset annual carbon storage at Monie Bay and Poplar Island by 0.7 and 2.1 percent, respectively, based

on average values of annual fluxes. However, there remains uncertainty in the accuracy of this estimate given the spatial and temporal variability in my observed fluxes, and the limited sampling frequency and spatial extent of my study. Within such uncertainty lays a justification for continued long-term monitoring of methane emissions in restored and natural marshes of Chesapeake Bay to resolve this important marsh management question.

# EVALUATING CARBON SEQUESTRATION POTENTIAL OF NATURAL AND RESTORED TIDAL MARSHES IN CHESAPEAKE BAY THROUGH QUANTIFICATION OF METHANE FLUXES AND IDENTIFICATION OF DRIVERS

by

Daniella Marie Hanacek

Thesis submitted to the Faculty of the Graduate School of the
University of Maryland, College Park, in partial fulfillment
of the requirements for the degree of
Master of Science
2022

Advisory Committee:
Dr. Lorie Staver and Dr. Jeffrey Cornwell, Chairs
Dr. Genevieve Noyce

# Acknowledgements

Funding for this work was provided by the Horn Point Laboratory and the NOAA Margaret A. Davidson Graduate Research Fellowship. Thank you to everyone who has helped along the way:

- My co-advisors Lorie Staver and Jeff Cornwell, as well as Mike Owens, for sharing their scientific expertise and providing guidance throughout my time as a student. Thanks especially for all of the encouraging meetings.
- Kyle Derby, my mentor through the Margaret A. Davidson Fellowship, for sharing enthusiasm for wetlands and providing advice on this research project.
- Dr. Genevieve Noyce who offered helpful suggestions on flux chambers and methane work and contributions as a committee member.
- The Chesapeake Bay National Estuarine Research Reserve, Maryland for hosting me as a fellow and welcoming me into the NERRS community, and the NOAA fellowship coordinators and leaders who made it possible.
- I am grateful to everyone who contributed in the field and lab: everyone at Poplar Island, CBNERR, Ben, Megan, Eli, Daniel, Mike, Lorie, Jeff.
- The students, staff, and faculty at Horn Point Lab and UMCES.
- Colleagues and friends from Dr. Tanner's SMP Lab at SMCM, MDE, NMSF, DNR, and Dr. Valiela's Lab and Ecosystems Center at MBL.
- Thank you to my Mom and Dad, my siblings, especially to my sister Natasha, all of my family and friends, and of course, to Daniel, for support and encouragement!

# Table of Contents

# List of Tables

# List of Figures

# Chapter 1

## *Introduction*

### *Global methane budget significance of wetlands*

Levels of atmospheric methane reached a record high in 2021 (Tollefson 2022, Lan et al. 2021), continuing the steady rise from the Industrial Revolution to the start of the 21$^{st}$ century, when levels showed relative stability until rapidly accelerating beginning around 2007 (Lan et al. 2021, Turner et al. 2019). This is a worrying trend, given that the global warming potential of methane is at least 28 times that of carbon dioxide (Tollefson et al. 2022, Lan et al. 2021). Using ice core measurements, scientists have attributed the bulk rise in methane concentrations since pre-industrial times to human activities: mainly increased agricultural development and the use of fossil fuels (Turner et al. 2019).

The cause of the 2007-onwards spike in methane emissions remains uncertain. The isotopic signature of methane shows that the 2007-onwards increase in methane levels corresponded to a decline in $\delta^{13}C\text{-}CH_4$, the ratio of heavy to light isotopes of carbon ($^{13}C/^{12}C$) as compared to the Pee Dee Belemnite standard (Lan et al. 2021, Nisbet et al. 2019). This has led to speculation that biogenic methane may be the cause of this rise in emissions, as microbially produced methane is depleted in the heavy isotope of carbon as compared to geologic and thermogenic associated methane synthesis (Tollefson 2022, Nisbet 2019, Lan et al. 2021, Whiticar 1999). Further examination of the hypothesis that biogenic sources are responsible for the isotopic shift identified tropical wetlands as a probable source – with increased methane emissions from tropical wetland ecosystems corresponding to climate change driven increases in precipitation and temperatures in the tropics (Lan et al. 2021, Nisbet et al. 2019). Conclusive identification of the source is hindered by challenges in mapping the areal extent of wetlands, the uncertainty in inundation area, and the need for regionally representative source signatures (i.e.

arctic wetlands emissions are approximately -68‰, whereas tropical wetland emissions are closer to -54‰) (Lan et al. 2021, Nisbet et al. 2019). Nevertheless, the accelerated pace of the rise in methane suggests that increased methane emission could be a consequence of global climate change, creating a positive feedback loop (Nisbet et al. 2019).

Predicting how climate change will impact the global methane budget requires an improved understanding of methane cycling in wetlands. In addition, improvements to bottom-up approaches of estimating global methane emissions to estimate source strength could be achieved by resolving why observations of emissions across aquatic habitats are so highly variable (Rosentreter et al. 2021). Briefly, bottom-up methods involve scaling empirical ground-based or model-based methane emission estimates by ecosystem area, whereas top-down methods utilize global distributions, atmospheric transport, $\delta^{13}C$ signatures, and $CH_4$ removal via the hydroxyl radical (but see Bridgham et al. 2012 for a more thorough explanation). Therefore, uncertainty within aquatic ecosystem types may be resolved, at least in part, with an improved mechanistic model of methane production and oxidation (Mostovaya et al. 2021, Rosentreter et al. 2021).

This has prompted calls for a robust data set of methane fluxes to be reported with relevant environmental data (Rosentreter et al. 2021). I address these needs by reporting a data set of methane fluxes along with relevant potential drivers from created and natural brackish marshes in Chesapeake Bay. While measurements of all useful environmental data to improve upscaling of results (water table, residence time, etc.) were beyond the scope of this project, the unique focus of my study site comparison of a marsh created with dredged sediment versus a marsh formed through ecological succession will advance both the goal of expanding the

empirical data set as well as the goal of defining successful restoration from a climatic perspective (Rosentreter et al. 2021).

*Blue carbon*

While wetlands are an atmospheric source of carbon from methane, they are also a valuable carbon sink. Wetland ecosystems are characterized by high rates of primary productivity. High rates of primary production, coupled with waterlogged, anoxic sediments that limit remineralization, result in the storage of large pools of organic carbon. Given this sequestration capacity, wetlands have the potential to act as important sinks in the global carbon cycle. This potential has led to the recognition that wetland organic matter storage can serve as a mechanism for reducing greenhouse gas (GHG) concentrations in the atmosphere, as the uptake of carbon dioxide ($CO_2$) during photosynthesis is assimilated into plant tissue and eventually retained as soil organic matter (Chmura et al. 2003, Bridgham et al. 2006, McCleod et al. 2011, Weston et al. 2014). Carbon sequestered by coastal ecosystems is referred to as blue carbon, and efforts have been made to create new wetlands or restore existing ones to enhance carbon sequestration (Kroeger et al. 2017, Macreadie et al. 2017).

The carbon sink capacity of wetlands, however, is diminished if methane and other GHG emissions exceed the rate of carbon fixation (Bridgham et al. 2006, McCleod et al. 2011, Chmura et al. 2016, Macreadie et al. 2019). While waterlogged conditions and high productivity enhance carbon storage, they can also fuel natural methane ($CH_4$) release (King and Wiebe 1978, Whiting and Chanton 1993, Megonigal and Schlesinger 1997).

The high global warming potential of $CH_4$ warrants further investigation into whether $CH_4$ can diminish wetlands as a carbon sink. Methane production is not well understood in oligohaline (salinity 0.5-5) or mesohaline (salinity 5-18) tidal marshes, where the abiotic controls

on production, such as sulfate inhibition, are more nuanced than in polyhaline marshes (salinity 18-30) (King and Wiebe 1980, DeLaune et al. 1983, Bartlett et al. 1987, Wang et al. 1996, Weston et al. 2006, Poffenbarger et al. 2011). As a result of high variability in GHG emissions, recent funding mechanisms for blue carbon restoration, including the Verified Carbon Standard Methodology for Tidal Wetland and Seagrass Restoration, currently exclude mesohaline marshes (Needelman et al. 2018).

*Biogeochemical controls on methane emissions*

Early studies on methane in wetlands established a role for seasonality, sulfate availability, salinity, and plant communities on methane fluxes. The highest emissions from a Georgia salt marsh were observed in August and September (King and Wiebe 1978). Observations in Louisiana and Virginia marshes provided early evidence that methane emissions in salt, brackish, and freshwater marshes were inversely related to sulfate and salinity (DeLaune et al. 1983, Bartlett et al. 1987). The explanation for the negative relationship between methane and salinity is based on the expected energetic favorability of sulfate-reducing bacteria over archaeal methanogens during anaerobic respiration. The abundance of sulfate in seawater, and consequent presence of sulfate ions in marsh sediments, allow sulfate-reducing bacteria to outcompete methanogens for energy sources in tidal marshes (DeLaune et al. 1983, Bartlett et al. 1987, Howes et al. 1985, Wang et al. 1996).

Recent studies suggest the proposed direct relationships between salinity, sulfate and methane emissions may not explain methane emissions in all tidal marshes (Poffenbarger et al. 2011, Weston et al. 2011, Ardon et al. 2018). Indeed, the idea of tipping points at which aquatic systems may undergo shifts in biogeochemical activity indicate that salinities of ~10-15 may be especially dynamic (Wang et al. 2017, Rosentreter et al. 2021). Increasing salinities could

influence methane production through the methanogen and sulfate reducer competition described above, but importantly could also influence the sediment microbial community via osmotic stress or changes in nutrient availability as a result of cation exchange or altered water sources (Wang et al. 2017). Abril and Iverson (2002) show overall calculated flux rates to the atmosphere were lower at a high salinity site in a fjord estuary than in freshwater or brackish sites, but that methane production exceeded oxidation of methane in the saltwater site, whereas the opposite was observed in the brackish site.

This thesis addresses controls of methanogenic activity in anoxic marsh sediments, recognizing there is a growing body of literature indicating methane production may occur in oxic environments and by other organisms including fungi and cyanobacteria (Liu et al. 2022, Rosentreter et al. 2021 and references therein, Grossart et al. 2011). Pioneering work on methane in the oxic mixed layer of the open ocean by Scranton (1972) revealed in-situ methane produced by coccolithophores and diatoms. Salt marsh sediments are frequently covered with a mat of microalgal or microbial assemblages – and thus $CH_4$ production could occur via alternative pathways.

*Chesapeake Bay marshes*

The mesohaline marshes of Chesapeake Bay are excellent sites for assessing controls on carbon cycling in tidal wetlands. Chesapeake Bay, the largest estuary in the United States, is home to approximately 282,000 acres of tidal wetlands ranging from tidal fresh to polyhaline (Baldwin et al. 2012, Chesapeake Bay Program 2019). The majority of the Chesapeake Bay is brackish with salinities below 20 (Baldwin et al. 2012). Chesapeake Bay marshes are threatened by sea level rise, with water levels in the Chesapeake Bay rising at an average 3.4 mm $yr^{-1}$, double the global average of 1.7 mm $yr^{-1}$ (Chesapeake Bay Sentinel Site Cooperative 2019).

Because of the importance of Chesapeake Bay wetlands as habitat for fish, waterfowl, mammals, and invertebrates, there is a strong interest in best management practices to protect these vital habitats (Baldwin et al. 2012, Chesapeake Bay Program 2019).

*Marsh creation*

Tidal marsh creation and restoration using dredged material ("beneficial use") represents a promising management practice for scientists and managers exploring the use of vegetated coastal habitats in eco-engineering approaches for climate mitigation and adaption (Staver et al. 2020). For example, the Paul S. Sarbanes Ecosystem Restoration Project at Poplar Island, uses dredged material from upper Chesapeake Bay navigation channels to create remote island habitat within the Chesapeake Bay. The first dredged material was placed in 2001 and, once construction is completed, the final project will consist of over 2.8 square kilometers of wetland habitat (USACE 2005). The restoration project provides habitat for local and migratory wildlife through both wetland and upland habitat. The success of the Poplar Island project could serve as a model for additional restoration projects in the region.

Quantification of the ecosystem service provided by created marshes is of interest to federal, state, and local entities that provide funding for restoration (Staver et al. 2020, Abbott et al. 2019). While ecological hysteresis can prevent the return to original ecosystems, marsh creation projects may result in ecosystems that have been rehabilitated if not entirely restored (Hemes et al. 2019). These wetlands can share some characteristics with natural sites, but may remain biogeochemically and ecologically unique (Hemes et al. 2019). For example, 150 years of modifications to the Sacramento-San Juaquin Delta have led Hemes and colleagues to argue that truly restoring the system to pre-industrial conditions is rendered impossible given changes to hydrology, salinity, plant community composition, and soil stocks (Hemes et al. 2019).

Notwithstanding any debate as to whether beneficial use marshes are to be considered restored or novel ecosystems, there remains a political will to do something useful with the $3.4 \times 10^6$ $m^3$ (4.5 mcy) of dredged material that needs placement annually. There is growing interest from scientists and managers over the potential of such projects as nature-based solutions to climate change (Staver et al. 2020, MDOTMPA 2018). Understanding the provisioning of ecosystem services, such as carbon sequestration, in these created marshes aids in determining their value. Furthermore, identifying environmental drivers of carbon sequestration may improve future planning of project design and implementation (Staver et al. 2020, Abbott et al. 2019). Prior research on long-term post-construction monitoring of restored or created marshes suggests there is an initial lag in the development of ecosystem services in created marshes before they resemble natural marshes (Craft et al. 2003). That observation prompted the following set of criteria for marsh restoration projects: " if wetland creation and restoration is to be successful at replacing wetland loss, it is important to know (1) how much time is needed for these ecosystems to achieve equivalence to natural wetlands and, (2) once equivalence is achieved, whether these ecosystems persist and provide long-term ecological benefits" (Craft et al. 2003).

Such criteria can be evaluated by measuring metrics of ecosystem function such as sedimentation, soil organic nitrogen, phosphorus and carbon accumulation, and soil organic carbon mineralization, as well as by ecological attributes including community structure (plant species composition), biomass, and producer-consumer activity (Staver et al. 2020, Cornwell et al. 2020, Abbott et al. 2019, Craft et al. 2003). This thesis contributes to the monitoring effort led by the University of Maryland Center for Environmental Science (UMCES) to gather long-term post-construction data in the marshes at Poplar Island. Here I report findings on methane cycling in one marsh cell, Cell 1A, which was 12-years post-construction at the time of this study.

Extensive evaluation of the monitoring metrics used by the UMCES researchers is reported elsewhere (see Staver et al. 2020, and Cornwell et al. 2020).

*Research objectives*

In this thesis I quantify methane effluxes from two Chesapeake Bay marshes, the created marshes at Poplar Island and the naturally occurring marshes at Monie Bay, a subcomponent of the Chesapeake Bay National Estuarine Research Reserve – Maryland. Poplar Island has been described in detail above, but an important additional consideration with this site is that because it was built from what were formerly Chesapeake Bay channel sediments, the oxidation of pyrite ($FeS_2$) can lead to high porewater sulfate ($SO_4^2$) concentrations (Cornwell et al. 2020). Accumulation of $SO_4^{2-}$ from $FeS_2$ is best expressed as the molar ratio of $SO_4^{2-}$ to $Cl^-$, with ratios above the expected seawater ratio of 0.052 indicating an enrichment of $SO_4^{2-}$ and lower ratios indicating sulfate reduction (Cornwell et al. 2020). At the time of initial construction, $SO_4^{2-}$ to $Cl^-$ ratios of Cell 1A, the site of this study, were well above 0.052 (Cornwell et al. 2020).

The Monie Bay component of the Chesapeake Bay National Estuarine Research Reserve-Maryland, is a well-studied marsh system, with past investigations of primary production (Stribling and Cornwell 1997), porewater nutrient profiles and plant biomass (Cornwell et al. 1994, Stribling et al. 2007), as well as marsh accretion (Zelenke and Cornwell 1996, Kearney et al. 1994) and responses to nutrient enrichment (Apple et al. 2004). Monie Bay is characterized as having relatively little human disturbance, providing a natural comparison to the marshes at Poplar Island.

As discussed, the restoration of marshes may lead to biogeochemically distinct systems with different patterns of carbon cycling than natural marshes. It is important then to understand how gaseous emissions from restored marshes compare to natural ones. In addition to measuring

methane fluxes, this thesis presents additional biogeochemical data that are useful for the interpretation of mechanisms responsible for the production and release of methane in mesohaline marsh sediments.

Relative to tropical wetlands, the total contribution of temperate wetlands to the global methane budget may be low, but they are still opportune systems in which to probe the dynamics of methane production and flux. The goal of such probing is to yield a better understanding of what variables control the production and transport of methane in aquatic ecosystems. Such information would improve global methane models and allow scientists to predict how aquatic ecosystems contribute to, and are regulated by, climate change.

This thesis examines wetland methane geochemistry, rather than atmospheric budgets. Observations at Poplar Island revealed bubbles of methane forming at the sediment surface (L. Staver, T. Kana, unpublished). This contradicts the notion that sulfate inhibits methane production, as there should be abundant sulfate present in sediments within these marshes, leading to the questions below.

Q1: What is the magnitude of $CH_4$ fluxes in created tidal marshes at Poplar Island?

Q2: How do they compare with natural tidal marshes of similar salinity, tidal range, etc.?

Q3: Are the drivers the same in the created and natural marshes?

Therefore, I present three hypotheses to be tested regarding the controls on methane emissions in Chesapeake Bay marshes.

H1: Mesohaline marshes in Chesapeake Bay function as carbon sinks, however this sink capacity is reduced by substantial fluxes of methane.

H2: Emissions of methane in restored mesohaline marshes will not exceed those in natural systems, given the lag time in the build-up of soil carbon stocks and availability of sulfate, both of which would limit available substrates for methanogenesis.

H3: Drivers of methane flux can be inferred from porewater chemistry.

These hypotheses are addressed through comparisons of $CH_4$ and $CO_2$ fluxes and porewater chemistry in the created marshes at Poplar Island and the natural marshes at Monie Bay.

***Methods***

The study sites were located at two marshes within the Chesapeake Bay (Fig. 1). Monie Bay (38°13'N, 75°51'W) is a tidal brackish embayment on the Wicomico River on the lower eastern shore of Maryland. The mean surface salinity range (1985-2021) for Monie Bay is 9.43-13.16 and the marsh is dominated by *Spartina alterniflora* with *Spartina cynosuroides*, *Spartina patens*, *Distichlis spicata* and *Juncus romerianus* also present (Chesapeake Bay Program 2022, Stribling et al. 2007). Estimates of Monie Bay marsh accretion suggest rates similar to rates of relative sea-level rise (Zelenke and Cornwell 1996, Chesapeake Bay Program 2022). Allochthonous inputs to fringe or submerged upland marshes, such as Monie Bay, are predominantly tidally driven as opposed to the fluvial trapping observed in marshes further upstream (Kearney and Stevenson 1994). Indeed, Monie Bay is characterized by organic-rich fine-grained sediments in back marsh areas. Poplar Island (38°76' N, 76° 38'W) is located in the mid-Bay main stem of Chesapeake Bay and the wetland restoration consists of a number of individual "cells" constructed using fine-grained sediment derived from navigation channels in the upper bay. The mean surface salinity range for the Chesapeake Bay mainstem at Poplar Island (1985–2021) is 8.89–16.13 (Chesapeake Bay Program 2021, Staver et al. 2020).

Fieldwork was conducted from May to December 2021 at Poplar Island and Monie Bay, focusing on the marsh vegetation growing season based on prior studies in the region that demonstrated a strong seasonality in fluxes with minimal $CH_4$ flux rates in the winter months (Derby et al. 2022, Noyce and Megonigal 2021). Fluxes of $CH_4$ were determined by measuring changes in concentration inside of static flux chambers placed over plants and the marsh sediment surface, following a modified version of Noyce and Megonigal (2021). Aluminum collars (1,600 $cm^2$) were inserted into the sediment to a depth of 15 centimeters. For access to the collars without disturbing the adjacent marsh platform during sampling events, boardwalk platforms were installed at Monie Bay in February 2021 and Poplar Island in March 2021 prior to the start of the study in May 2021. Six collars were inserted at both sites; 3 each in the high and low marsh plant community zones. At Poplar Island the high marsh vegetation was dominated by *S. patens*, *D. spicata*, and *Pluchea odorata,* and the low marsh by *S. alterniflora.* At Monie Bay, the high marsh was dominated by *S. patens* and *D. spicata*, though there was considerable growth of *S. alterniflora*, and the low marsh was primarily covered with *S. alterniflora*. During sampling events, clear chambers (40 cm × 40 cm × 40 cm) were attached to the collars and sealed with a foam gasket and clamps. Plant height at the peak of the growing season required the stacking of two (height of 80 cm) to three (120 cm) chamber sections to avoid plant disturbance. Temperature inside each chamber was monitored during the sampling period with Hobo temperature data loggers (Pro v2, Onset Corp.).

The $CH_4$ fluxes were determined by withdrawing five gas samples into 12mL glass vials (Labco Exetainer®,Lampeter, Wales, UK) from each chamber over the course of at least 1 hour. Gas samples were analyzed within 24 hours of sampling using a Shimadzu Gas Chromatograph with a flame ionization detector. Fluxes were calculated as the change in methane concentration

in the chamber headspace over the 5 time points. Annual estimates of methane flux at Poplar Island and Monie Bay were calculated by using the monthly fluxes in June, July, August and September, to represent the months of the growing season that both sites were sampled, as an upper limit to annual fluxes. It is expected that $CH_4$ fluxes in winter months of the year would not exceed the growing season fluxes, and so our estimate is given as an upper limit of expected fluxes.

Seasonal porewater dissolved $CH_4$, $CO_2$, and nutrients were measured using porewater equilibrators (Hesslein 1976). Six equilibrators were installed to a depth of approximately 15cm at both sites at least two weeks prior to each gas flux chamber sampling event. Equilibrators corresponded to flux chamber locations; 3 each in the high and low marsh, though exact placement in the marsh was changed per each sampling to ensure sediments sampled were not affected by prior insertion. On the same day as flux chamber sampling occurred, equilibrators were retrieved from the sediment and processed in the field. Porewater was extracted from each well using a 10mL syringe. Samples were split into Exetainer vials® for analysis of dissolved methane and carbon dioxide, and into plastic vials for porewater sulfate/chloride, dissolved iron, and nutrient analyses. Nutrient samples were filtered and kept on ice pack until returning to the lab and then frozen until later analysis. Dissolved gas samples were promptly analyzed upon return to the lab by shaking vigorously to allow dissolved gases to come to equilibrium before they were analyzed on a gas chromatograph. Soluble reactive phosphorus and ammonium were analyzed colorimetrically (Parsons et al. 1984), dissolved Fe was analyzed using Ferrozine colorimetry (Gibb 1979), and sulfate and chloride were analyzed after dilution on an ion chromatograph (Cornwell et al. 2020). Statistical and graphical analyses were performed using R statistical software (v4.1.3; R Core Team 2022).

***Results***

*Carbon flux measurements*

Mean rates of site-average methane emission ranged from 2,315 μmol $CH_4$ $m^{-2}$ $d^{-1}$ observed in the low marsh of Poplar Island in July to -415 μmol $CH_4$ $m^{-2}$ $d^{-1}$ in the low marsh of Monie Bay in December (Fig. 2). The $CH_4$ flux at Poplar Island in July had a standard error of 1,532 μmol $CH_4$ $m^{-2}$ $d^{-1}$, and could likely be attributed to an ebullition event during that sampling. Even so, half of the sampling dates did have a standard error exceeding 100 μmol $CH_4$ $m^{-2}$ $d^{-1}$, indicating high spatial variability over short distances. Mean growing season methane emissions were -33.3 ± 65.1 μmol $CH_4$ $m^{-2}$ $d^{-1}$ from the Poplar Island high marsh, 1,005.7 ± 554.1 μmol $CH_4$ $m^{-2}$ $d^{-1}$ from the Poplar Island low marsh, 94.4 ± 72.1 μmol $CH_4$ $m^{-2}$ $d^{-1}$ from the Monie Bay high marsh, and 203.1 ± 109.3 μmol $CH_4$ $m^{-2}$ $d^{-1}$ from the Monie Bay low marsh (Fig. 3.). There was no significant difference in the growing season methane flux between Poplar Island and Monie Bay (t-test, $p>0.05$). Fluxes over the study period were highly variable with the largest fluxes occurring mid to late summer (Fig. 4).

Mean rates of site-average carbon dioxide exchange ranged from -1,344.5 mmol $CO_2$ $m^{-2}$ $d^{-1}$ in the low marsh of Monie Bay in October to 173.5 mmol $CO_2$ $m^{-2}$ $d^{-1}$ in the low marsh of Monie Bay in December (Fig. 5.). Mean growing season carbon dioxide emissions were 1.2 ± 53.1 mmol $CH_4$ $m^{-2}$ $d^{-1}$ from the Poplar Island high marsh, -95.2 ± 113.4 mmol $CH_4$ $m^{-2}$ $d^{-1}$ from the Poplar Island low marsh, -43.5 ± 31.5 mmol $CH_4$ $m^{-2}$ $d^{-1}$ from the Monie Bay high marsh, and -162.3 ± 130.4 mmol $CH_4$ $m^{-2}$ $d^{-1}$ from the Monie Bay low marsh (Fig. 6). $CO_2$ exchange did not show strong seasonal trends (Fig. 7).

*Porewater analyses*

The low marsh $CH_4$ concentrations at Poplar Island exceeded those in the high marsh, whereas high and low marsh sites at Monie Bay show comparable concentrations and gradients (Fig. 8). The highest concentrations were observed below 9cm depth. Averaged dissolved methane concentrations in the top 15 cm of interstitial water of marsh sediments show a high degree of seasonality (Fig. 9). Methane concentrations peaked in the warmer months of the summer and declined through the fall, yet remained higher in December at the completion of my study period than at its beginning in May (Fig. 9). Seasonal changes in the soil methane pool aligned with the seasonality observed in the methane flux (Fig. 9). The pore water methane concentrations appear to ramp up faster and remain high later into the year in the low marsh of Poplar Island, showing high values early in the growing season in May and June; however, the highest concentrations were observed at Monie Bay at the end of August (Fig 9). Poplar Island low marsh sites had concentrations similar to those observed in the high and low marsh at Monie Bay, whereas values in the high marsh at Poplar Island remained low through the growing season, exhibiting only a slight peak at mid-summer (Fig. 9).

Porewater dissolved methane, carbon dioxide, iron, ammonium, soluble reactive phosphorus, and sulfate-to-chloride ratios averaged over the top 15 cm are shown in Table 1 and Table 2. Note that some averages do not include data for the uppermost layer sampling wells because they were dry. Seasonal trends in pore water constituents are seen in Fig. 10. There appears to be stronger coupling between Fe and SRP in the low marsh at Poplar Island than Monie Bay, likely resulting from the increased abundance of solid phase Fe in the created marshes than in the natural marshes and interactions between the two constituents (Cornwell et al. 2020).

Porewater concentrations of $CH_4$ and $SO_4^{2-}$ were expected to show an inverse relationship (Bartlett et al. 1987 and references therein), and my data support such coupling between methanogenesis and sulfate reduction (Fig. 11). As Crill and Martens (1983) and Bartlett et al. (1987) demonstrated early on, methanogenesis can shoal upwards in the sediment profile when sulfate concentrations decline due to increased rates of sulfate reduction. This occurred in August at Monie Bay and July and September at Poplar Island (noting that the August value at MB was obtained on August 31st and the September value for PI was obtained on September 2nd) (Fig. 11). However, average sulfate to chloride molar ratios and dissolved methane did not show a strong linear correlation, as might be predicted if sulfate availability was the only control on methane flux (Fig. 12). Furthermore, while sulfate to chloride ratios tend to be higher at depth at Poplar Island than at Monie Bay, high concentrations of dissolved methane were also observed in these interstitial waters (Figs. 7, 13).

## ***Discussion***

### *Restored versus natural marshes*

In their study of subtropical southwest Florida restored and created freshwater and brackish marshes, and natural freshwater marshes, Li and Mitsch (2016) hypothesized that both restored/created marshes will have lower methane emissions than a natural freshwater reference site. In contrast, they found both restored sites had higher fluxes than the natural site with the mean methane emissions from the restored freshwater site 124 g $CH_4$-C $m^{-2}$ $yr^{-1}$, as compared to 0.8 g $CH_4$-C $m^{-2}$ $yr^{-1}$ at the natural site. Their study demonstrates that the mechanisms controlling methane dynamics in restored and built wetlands are complicated by the management regime (hydrology) and time scale of research (years of wetland development). They propose that from a

methane management perspective, created and restored marshes should minimize deep-water areas. In my study, the difference between high and low marsh sites for both methane flux and porewater methane concentrations at Poplar Island appeared to be greater than the observations from Monie Bay (Fig. 9.). This could be driven by plant community composition or inundation frequency and duration, as I observed *S. alterniflora* in the high marsh of Monie Bay but not Poplar Island. This implies that marsh construction strategies need to consider the proportion of high and low marsh and marsh hydrology if methane emission reduction is a management goal. In created riparian wetlands in Ohio, Altor and Mitsch (2006) described challenges associated with both the hydrology and the observation time scale for restoration studies. Average methane flux rates of 13 to 42 g $CH_4$-C $m^{-2}$ $yr^{-1}$ from 10-year-old created wetlands fell near what was expected for swamps and marshes of similar latitudes, around 35 $CH_4$-C $m^{-2}$ $yr^{-1}$ (Bartlett and Harris 1993, in Altor and Mitsch 2006). This suggests that within a decade, carbon cycling in created riparian wetlands resembled that of natural systems.

The methane cycling in the 12-year-old restored marsh at Poplar Island had similar porewater methane concentrations and flux rates found in the natural marshes of Monie Bay (Fig. 9). How our 12-year-old marsh compares to other marshes within the chronosequence of development will have important implications regarding the timeframe in which restoration projects return to expected biogeochemical cycling. Craft et al. (2003) demonstrated the eventual return of elemental cycling processes following an initial lag post-wetland creation and/or restoration. This trend is supported by findings from a pilot study of methane fluxes at Poplar Island by Staver et al. (2020) showing a lag of 10 years may be expected. The restoration of carbon cycling processes in created systems was also investigated by Abbott and others (2019) in a study of created marshes of the Sabine National Wildlife Refuge on the Chenier Plain in

Southwest Louisiana. There, as hypothesized, carbon stocks increased with age in created wetlands to within 8% of those expected in natural wetlands in a 32-year-old marsh. Differences between short- and long-term carbon accretion rates between marshes of different age likely has a large impact on net C balance. This suggests non-linearity in the trajectory of marsh development – a reality of marsh restoration projects which demonstrates the need for long-term monitoring of carbon cycling processes over chronosequences of marsh development.

As noted previously, Craft et al. (2003) also advocated for long-term monitoring of post-construction marsh creation, based upon the observation of an initial lag in the provisioning of ecosystem services in created marshes before they resemble natural systems they were designed after. In a study of marshes built from dredged sediments in coastal North Carolina and nearby reference marshes, these workers found that soil carbon pools were slow to develop even after almost 30 years, but at least one 24-year-old constructed marsh resembled carbon stocks at its paired reference site. And by 8 years, soil organic carbon pools in the created marshes began to fall within the range of values observed across natural reference sites. Working in this same system, Cornell et al. (2008) found that methane contributed minimally to microbial respiration in these high salinity marshes, but that the major carbon fluxes were established in built marshes within five years of development. They contend that the rapid development of marsh gas exchange in created marshes, as compared to annual plant production, warrants increased attention given possible feedbacks between plant physiology and ecosystem function.

While this study is limited to the findings of a 12-year-old marsh at Poplar Island, the results fall within the predicted range of methane flux based on the expected linear increase in flux across the chronosequence of marsh age in sediment core incubations as reported in Staver et al. (2020). Linear interpolation yields an estimate for methane production at 78 mg $CH_4$ $m^{-2}$ $d^{-1}$

for a marsh of 12 years of age. On a yearly basis, if all the expected methane was released that would lead to a flux rate of 28.47 g $CH_4$ $m^{-2}$ $yr^{-1}$. My results indicate an upper bound of methane flux (based on the low marsh growing season average) for a marsh of this age to be approximately 25 g $CH_4$ $m^{-2}$ $yr^{-1}$ (based on the average + 1 se). The measured fluxes in this study and the flux rate based on linear interpolation by Staver et al. (2020) are indeed comparable, demonstrating that future flux chamber experiments across the chronosequence could confirm the sediment core predictions.

Tidally restored wetlands in the San Francisco Bay Delta emitted 0.62-0.2 g $CH_4$-C $m^{-2}$ $yr^{-1,}$ while young non-tidal managed wetlands emitted 44 g $CH_4$-C $m^{-2}$ $yr^{-1}$ and old non-tidal managed wetlands emitted 37 g $CH_4$-C $m^{-2}$ $yr^{-1}$ (Arias-Ortiz et al. 2021). Differences were observed between the restored tidal and non-tidal wetlands, but not within the two non-tidal systems. On a kilogram to kilogram comparison, the ratio of $CO_2$ sequestration to $CH_4$ emission was found to be highest in the tidal system at 310:1 (kg:kg), 17:1 in the young non-tidal, and 24:1 in the older non-tidal. Tidal wetland restoration resulted in a negative radiative forcing as a result of increased soil C accumulation, while non-tidal restoration exhibited early positive forcing based on increased methane emissions potentially lasting from 1 year to 12 decades. They caution though, that the actual effect of wetland restoration actions on climate forcing is not measured by wetland radiative balance but rather by the net change of that balance from pre-restoration land-use. Agreeing on the need for other metrics of restoration success on climate forcing, Holm. Jr. and colleagues (2016) made the case that the benefits of restoring wetlands in the Mississippi delta for climate regulation hinges less on the annual carbon sequestration benefits than on preventing the losses of existing wetland area. Given that such losses would

result in the erosion and emissions of upwards of a meter, or a century's worth, of buried soil carbon (Holm Jr. et al. 2016).

The benefits of marsh conservation and restoration are more nuanced than a snapshot of a marsh carbon budget will allow. Even so, I calculated how these measured fluxes of methane would offset carbon storage. I found that approximately 0.7 to 2.1% of the annual carbon buried in the sediments may be lost as methane efflux based on average flux rates at Monie Bay and Poplar Island, respectively (Table 3). My results fall into the lower range of estimates from a recent meta-analysis by Rosentreter et al. (2021), which found methane emissions from coastal salt marshes can account for up to 25% of long-term carbon burial in these systems (Table 3). In addition, when the same calculations are made for the tidal freshwater marsh system of Jug Bay, an embayment on Maryland's Patuxent River, 29% of annual carbon storage is released as methane (Table 3). I would expect that system to yield greater losses to methane given the limited availability of sulfate, but it also falls near that 25% range reported in the review above. If we think about these offsets in terms of the global warming potential (GWP) of methane on a 100 year timeframe (27 at the lower end), and not just percent of carbon, the methane efflux based on averages at Monie Bay and Poplar Island lead to 17.9 and 57.9 percent of $CO_2$ stored being offset as gaseous emissions of methane. However, these are sustained fluxes and there is some question as to the suitability of GWPs as a metric in quantifying the climactic role of ecosystems (Neubauer and Megonigal 2015).

*Potential drivers of methane flux*

When I compared the measured fluxes to their corresponding porewater values, I found that pore water concentrations may not be the best predictor of flux (Fig. 14.). Other studies suggest observed fluxes do not always reflect what would be expected from porewater gradients.

I calculated diffusive fluxes of methane based on the sediment porewater concentrations to determine if this discrepancy exists at our sites using Fick's First Law, J= ΦDdC/dz (Kelley et al. 1995, Berner 1980). The flux rates measured with static flux chambers are greater than would be expected owing strictly to diffusion gradients (Fig. 15).

I expected that sulfate availability should limit the concentrations of methane in sediment porewaters given the widely cited relationship between sulfate reduction and methanogenesis discussed previously. My data support sulfate reduction as a limiting process for methanogenesis, and ultimately flux rates (Figs. 11,12). The differences between the observed and expected fluxes, however, imply that biological or geochemical drivers unrelated to salinity also act as controls on methane. In their study on the Alabama coast, Wilson et al. (2015) hypothesize that wetland sites within Weeks Bay (salinity of 3.8) and Dog River (salinity 5.1) should exhibit fluxes of methane 13 to 16 times, respectively, those of Dauphin Island (salinity 24.5). Instead, they found that Weeks Bay fluxes were only 1.9 times those of Dauphin Island, and little difference exists between Dauphin Island and Dog River. Wilson and colleagues attribute the discrepancy between observed fluxes and expected fluxes to methane oxidation and hydrology. Kelley et al. (1995) also found such a discrepancy between fluxes measured from static flux chambers with estimated fluxes based upon porewater gradients. In that instance, chamber measurements showed higher fluxes than could be expected from diffusional gradients. Those workers suggest plant-mediated transport as one explanation (Kelley et al. 1995).

The high rates of carbon assimilation in wetland plants and the ability of plants to act as a conduit for $CH_4$ flux (Dacey and Klug 1979) lead to questions of how plant biomass controls methane emissions. For example, plants could control emissions by supplying carbon to microbial methanogens, by supplying oxygen to the rhizosphere and associated methane

oxidation, and by transporting the produced methane, or some combination of these. An increase in biomass could allow for greater transport of methane from soils by increasing the volume of porous vascular tissue and, consequently, the quantity of $CH_4$ transported (Megonigal and Schlesinger 1997).

If methanogenesis is limited by the availability of labile organic carbon compounds in the sediments, then increases in plant biomass could lead to elevated $CH_4$ emissions. Increased leaf and root materials and enhanced root exudation of labile organic carbon could increase microbial activity (Megonigal and Schlesinger 1997, Pastore et al. 2017). Observations along the Patuxent River estuary from brackish to freshwater marshes (Neubauer et al. 2005) suggested that brackish sites had more soil organic matter and lower rates of microbial respiration than freshwater sites. That study concluded that the detritus from brackish marsh species was more refractory than from freshwater marsh species and that differences in organic matter content could be more important than decomposition pathways (Neubauer et al. 2005). The transfer of plant material to sediments and resulting methanogen use of plant-derived carbon was hypothesized to increase with ecosystem production. However, this was not found to be true in a study conducted in Delaware Bay (Weston et al. 2014). Accordingly, how wetland plant growth is related to increased methane emissions through root exudation and turnover of usable carbon, needs to be further explored.

Stribling and Cornwell (1997) measured aboveground annual *S. alterniflora* biomass in a creek bank marsh at Monie Bay to be 320 grams dry weight per meter squared while *S. alterniflora* biomass for the studied marsh at Poplar Island is estimated in the range of 900-1,350 grams dry weight per meter squared based on the biomass monitoring of Staver et al. (2020). I did not observe a difference in methane emissions during the growing season for the *S.*

*alterniflora* dominated low marsh zones, as the standing stock of biomass was changing, indicating biomass alone does not explain emissions. However, belowground biomass may be important in driving differences in root oxidation and these aboveground measurements do not reflect the spatial variability of my sampling locations. In addition, the availability of a usable versus refractory carbon pool could vary between the two marsh systems and could represent a more indirect control by plant biomass on methane emissions.

### *Conclusion*

This thesis demonstrates that growing season methane fluxes from a 12-year-old restored marsh at Poplar Island are similar to those from a natural marsh, Monie Bay. Methane fluxes exhibited strong seasonality at the two Chesapeake Bay marshes, as expected. The highest methane fluxes were observed in July at Poplar Island and in August at Monie Bay. The data in this thesis do not have the statistical power needed to demonstrate spatial trends, however the difference in porewater methane concentrations and flux rates between the high and low marsh zones at Poplar Island is greater than in the two zones at Monie Bay. This is likely due to elevational differences, with the high marsh at Poplar Island constructed at a higher elevation than observed in natural high marshes of the region.

Porewater methane concentrations in the low marsh at Poplar Island match those observed at Monie Bay, indicating a return of carbon cycling process in the restored marsh. Porewater methane exhibited a similar seasonality to fluxes, with methane concentrations generally higher during the growing season. However, there were some exceptions. For example, the highest overall dissolved methane concentration observed at Poplar Island was at the 15cm depth in December. Correlations between sulfate concentrations and methane concentrations in

marsh porewater were less robust than expected, suggesting some other non-salinity drivers may be important for methane production in these marshes. Measurements of iron, soluble reactive phosphorus, and ammonium did not show any strong control on methane concentrations or methane fluxes.

The carbon sequestration benefit of the mesohaline Chesapeake Bay marshes is partially offset by emissions of methane in the range of 0.7-2.1% of carbon stored, based on the average values reported in this thesis. While this project was limited to two sites, it suggests that a more thorough field campaign across greater spatial and temporal scales is warranted to adequately inform management decisions around this topic. It confirms the need for continued long-term monitoring of carbon cycling processes, including methane effluxes, biomass sampling, and carbon accumulation, to refine future assessments of the blue carbon potential of these ecosystems.

Tables

Table 1. Average porewater dissolved solute concentrations ± standard error of the mean and ratios in the upper 15cm of marsh sediments at Poplar Island.

| | Date | Fe (mg $L^{-1}$) | SRP (µM) | NH4 (µM) | $SO_4^{2-}$: $Cl^-$ | $CH_4$ (µmol $L^{-1}$) | $CO_2$ (mol $L^{-1}$) |
|---|---|---|---|---|---|---|---|
| High marsh | 5/3/2021 | 8.6 ± 2.5 | 30.2 ± 4.3 | 52.8 ± 7.6 | 0.05 ± 0.01 | 1.0 ± 0.3 | 0.03 ± 0.004 |
| | 6/23/2021 | 8.7 ± 1.6 | 21.3 ± 0.8 | 118.5 ± 13.8 | 0.06 ± 0.04 | 0.33 ± 0.1 | 0.06 ± 0.01 |
| | 7/13/2021 | 19.9 ± 9.9 | 36.6 ± 6.9 | 660.5 ± 214.7 | 0.08 ± 0.01 | 5.3 ± 3.7 | 0.05 ± 0.01 |
| | 9/2/2021 | 22.1 ± 9.4 | 10.1 ± 1.6 | 256.2 ± 53.0 | 0.03 ± 0.02 | 6.4 ± 2.9 | 0.04 ± 0.01 |
| | 10/7/2021 | 24.3 ± 10.3 | 11.3 ± 2.3 | 110.9 ± 28.8 | 0.01 ± 0.01 | 2.1 ± 1.5 | 0.08 ± 0.03 |
| | 12/15/2021 | 25.8 ± 12.3 | 39.8 ± 15.1 | 129.1 ± 36.5 | 0.04 ± 0.01 | 6.4 ± 2.4 | 0.02 ± 0.01 |
| Low marsh | 5/3/2021 | 7.8 ± 2.8 | 78.3 ± 26.2 | 133.1 ± 18.1 | 0.08 ± 0.01 | 56.1 ± 26.7 | 0.02 ± 0.01 |
| | 6/23/2021 | 73.5 ± 9.6 | 53.0 ± 8.5 | 95.7 ± 8.3 | 0.05 ± 0.004 | 61.2 ± 18.3 | 0.02 ± 0.004 |
| | 7/13/2021 | 70.2 ± 10.6 | 124.3 ± 16.7 | 141.7 ± 16.8 | 0.05 ± 0.01 | 95.1 ± 20.4 | 0.1 ± 0.01 |
| | 9/2/2021 | 35.8 ± 9.1 | 143.7 ± 22.5 | 177.4 ± 39.8 | 0.05 ± 0.01 | 144.9 ± 16.7 | 0.06 ± 0.01 |
| | 10/7/2021 | 26.7 ± 10.4 | 73.2 ± 13.8 | 79.2 ± 19.1 | 0.04 ± 0.003 | 167.0 ± 21.9 | 0.1 ± 0.02 |
| | 12/15/2021 | 9.2 ± 3.4 | 50.6 ± 18.6 | 35.0 ± 7.3 | 0.04 ± 0.01 | 137.9 ± 40.5 | 0.02 ± 0.003 |

Table 2. Average porewater dissolved solute concentrations ± standard error of the mean and ratios in the upper 15cm of marsh sediments at Monie Bay.

| | Date | Fe (mg $L^{-1}$) | SRP (µM) | NH4 (µM) | $SO_4^{2-}$: $Cl^-$ | $CH_4$ (µmol $L^{-1}$) | $CO_2$ (mol $L^{-1}$) |
|---|---|---|---|---|---|---|---|
| High marsh | 6/7/2021 | 37.5 ± 14.1 | 31.9 ± 4.8 | 138.7 ± 36.3 | 0.04 ± 0.01 | 11.2 ± 6.2 | 0.05 ± 0.01 |
| | 7/22/2021 | 0.03 ± 0.2 | 37.2 ± 5.1 | 180.0 ± 34.3 | 0.01 ± 0.001 | 98.5 ± 40.7 | 0.17 ± 0.02 |
| | 8/31/2021 | 0.3 ± 0.1 | 16.7 ± 1.9 | 95.4 ± 20.3 | 0.02 ± 0.004 | 153.8 ± 23.6 | 0.22 ± 0.05 |
| | 10/14/2021 | 2.6 ± 0.3 | 23.1 ± 2.5 | 163.2 ± 24.1 | 0.05 ± 0.004 | 143.1 ± 29.2 | 0.06 ± 0.01 |
| | 12/7/2021 | 4.1 ± 0.3 | 5.9 ± 0.9 | 50.2 ± 5.4 | 0.04 ± 0.002 | 36.6 ± 22.7 | 0.01 ± 0.001 |
| Low marsh | 6/7/2021 | 5.2 ± 2.7 | 44.8 ± 17.5 | 115 ± 30.0 | 0.07 ± 0.001 | 11.9 ± 8.3 | 0.02 ± 0.01 |
| | 7/22/2021 | 10.4 ± 5.2 | 35.1 ± 7.3 | 138.0 ± 30.5 | 0.05 ± 0.02 | 134.4 ± 40.4 | 0.04 ± 0.01 |
| | 8/31/2021 | 1.0 ± 0.4 | 22.0 ± 2.1 | 65.8 ± 15.0 | 0.02 ± 0.01 | 206.4 ± 13.7 | 0.07 ± 0.01 |
| | 10/14/2021 | 11.7 ± 3.8 | 30.8 ± 7.3 | 139.6 ± 39.4 | 0.05 ± 0.01 | 123.7 ± 33.6 | 0.04 ± 0.01 |
| | 12/7/2021 | 22.8 ± 7.8 | 19.4 ± 3.1 | 75.2 ± 7.2 | 0.03 ± 0.01 | 61.0 ± 26.5 | 0.01 ± 0.001 |

Table 3. Carbon sequestration and methane fluxes at Monie Bay and Poplar Island in comparison to lower and higher salinity systems.

| Site | Site description | Average N burial rate (g N $m^{-2}$ $y^{-1}$) | C:N ratio | Average C burial (g C $m^{-2}$ $y^{-1}$) | Average $CH_4$ flux* (g C-$CH_4$ $m^{-2}y^{-1}$) | Median $CH_4$ flux* (g C-$CH_4$ $m^{-2}y^{-1}$) | % of C burial lost to $CH_4$ flux based on average | % of C burial lost to $CH_4$ flux based on median |
|---|---|---|---|---|---|---|---|---|
| Monie Bay[a] | Brackish | 10.6 | 12.8 | 135.7 | 0.9 | 0.45 | 0.7% | 0.3% |
| Poplar Island[b] | Restored/created brackish | 10.4 | 19.8 | 206 | 4.42 | 1.87 | 2.1% | 0.9% |
| Jug Bay[cd] | Tidal Freshwater | 21.4 | 12.5 | 267.5 | 78.6 | -- | 29.4% | -- |
| Global estimate for coastal salt marshes[e] | Salt marsh | -- | -- | 2.0-1,712.9 | -0.41- 413.4 | -- | 0-25% | -- |

[a]Monie Bay C burial rates from Merrill 1999, based on reported C:N ratio
[b]Poplar Island C burial rates from Staver et al. 2020; N burial rates from Staver et al. 2021
[c]Jug Bay C burial rates from Merrill 1999
[d] Jug Bay methane flux rates from Keller et al. 2013
[e] Meta-analysis of global coastal salt marshes by Rosentreter et al. 2021
*Comparisons only include low marsh growing season (June-Sept in this study) methane fluxes as the C burial rates correspond to the low marsh of the two sites

Figures

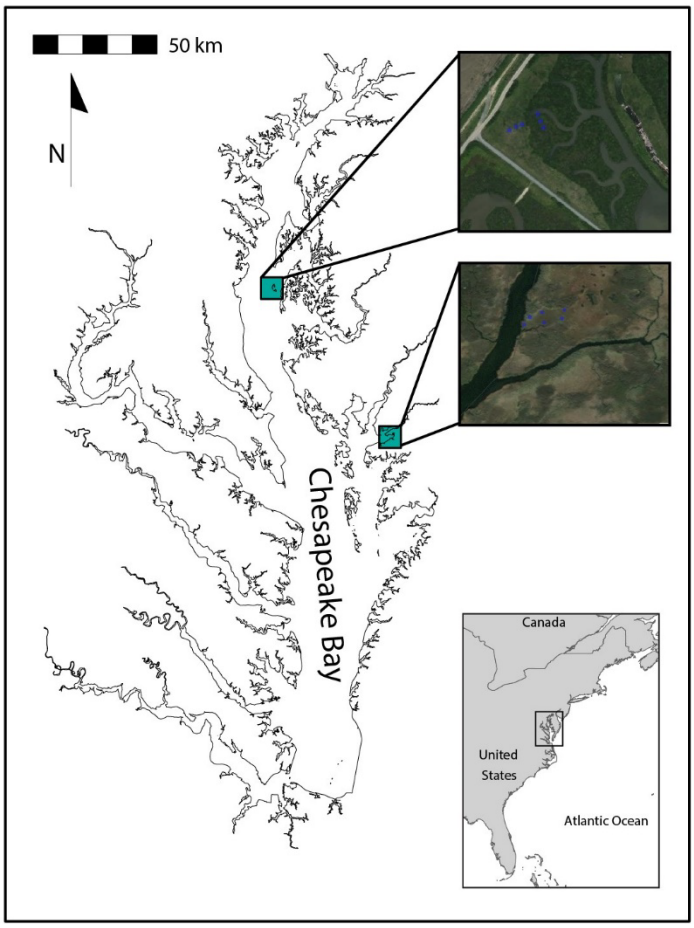


Figure 1. Study site locations in the Chesapeake Bay with insets showing Poplar Island (upper) and Monie Bay (lower), and the location of Chesapeake Bay estuary on the US East Coast.

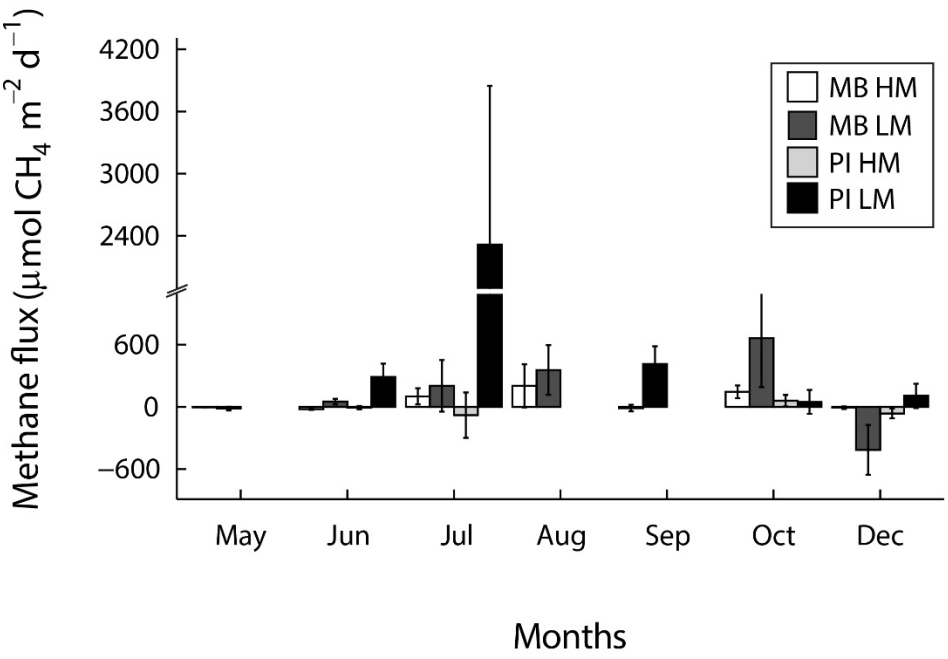


Figure 2. Methane fluxes measured in the high and low marsh zones of Monie Bay and Poplar Island for each month of sampling. Error bars represent standard error of the mean fluxes. Positive fluxes are out of the sediment.

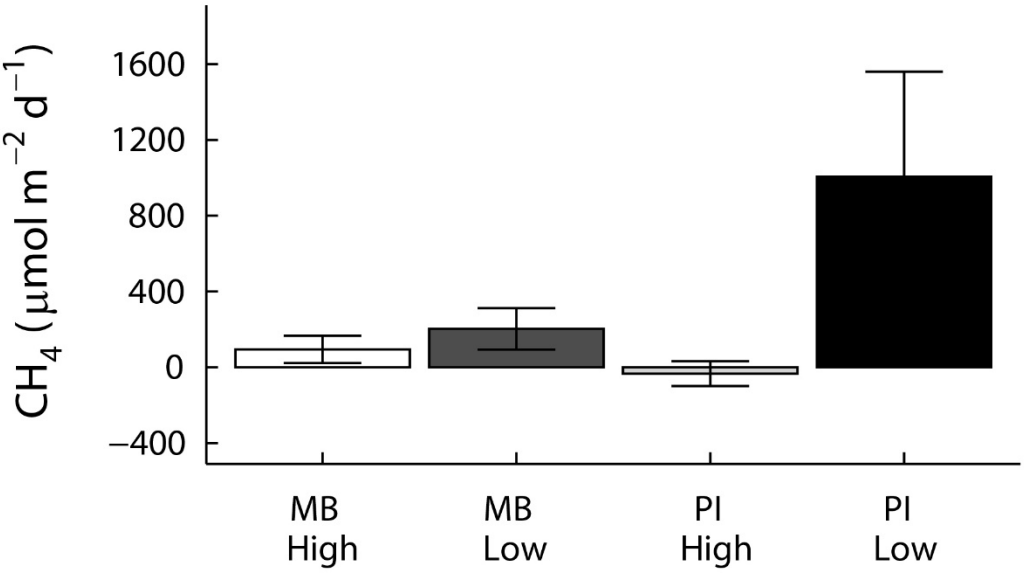


Figure 3. Methane fluxes averaged across the growing season in the high and low marsh zones of Monie Bay and Poplar Island. Error bars represent standard error of the mean fluxes.

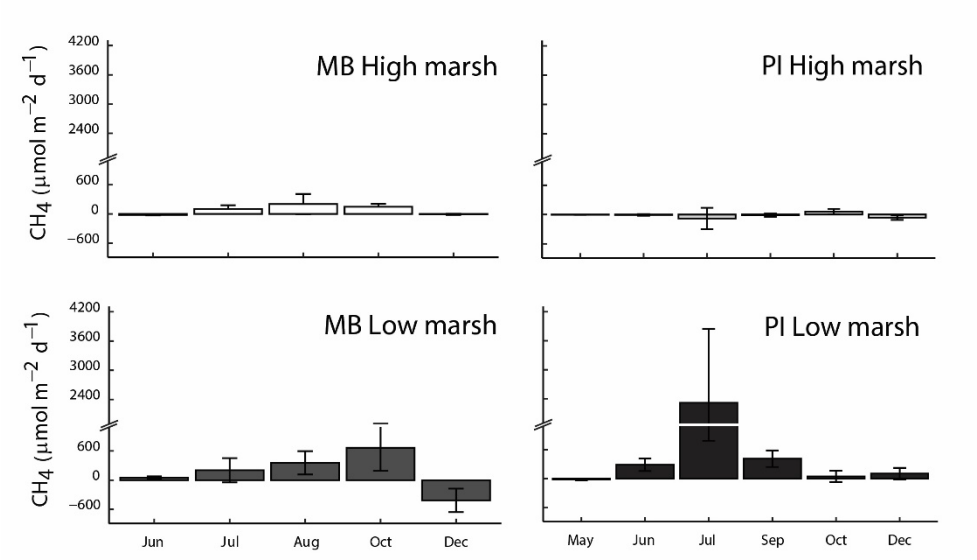


Figure 4. Methane fluxes measured at Monie Bay and Poplar Island for each month of sampling split into panels per marsh and vegetation zone. Error bars represent standard error of the mean fluxes. Positive fluxes are out of the sediment.

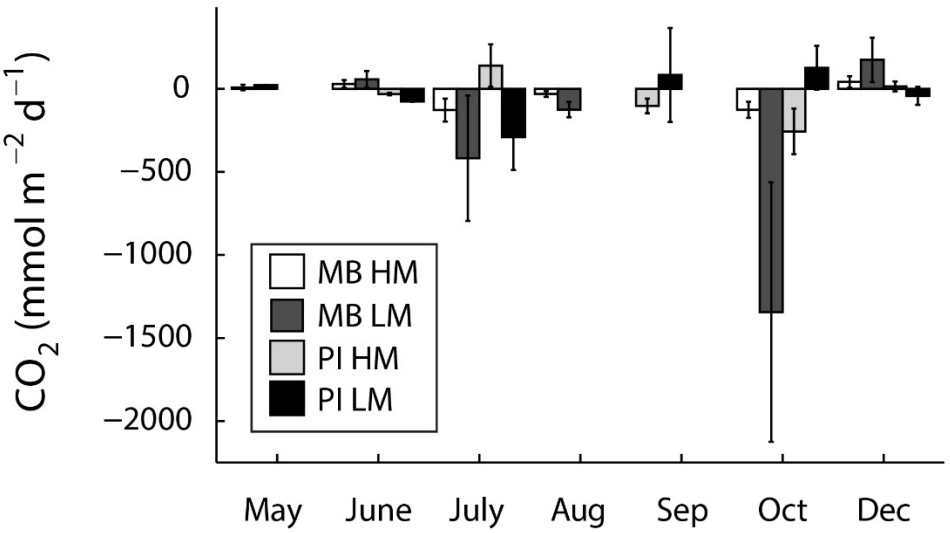


Figure 5. Carbon dioxide fluxes measured in the high and low marsh zones of Monie Bay and Poplar Island for each month of sampling. Error bars represent standard error of the mean fluxes. Positive fluxes are out of the sediment.

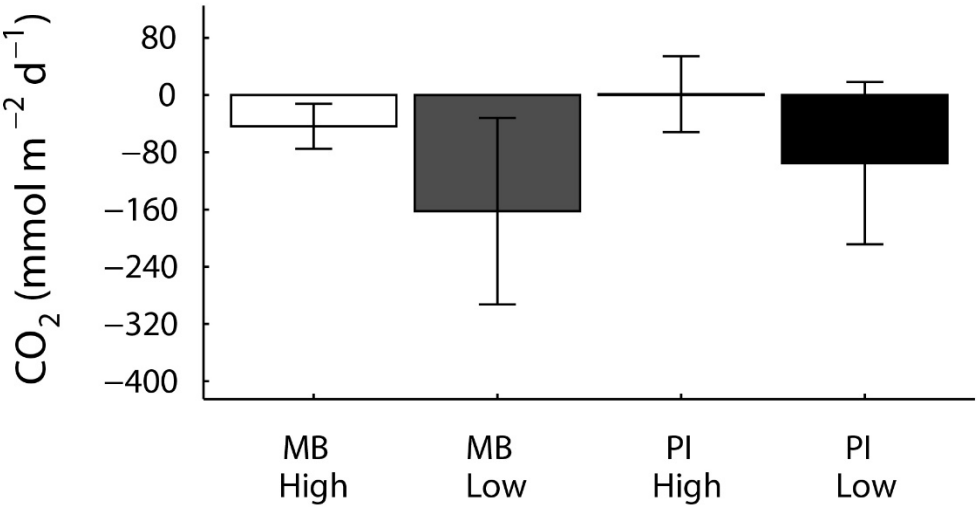


Figure 6. Carbon dioxide fluxes averaged across the growing season in the high and low marsh zones of Monie Bay and Poplar Island. Error bars represent standard error of the mean fluxes.

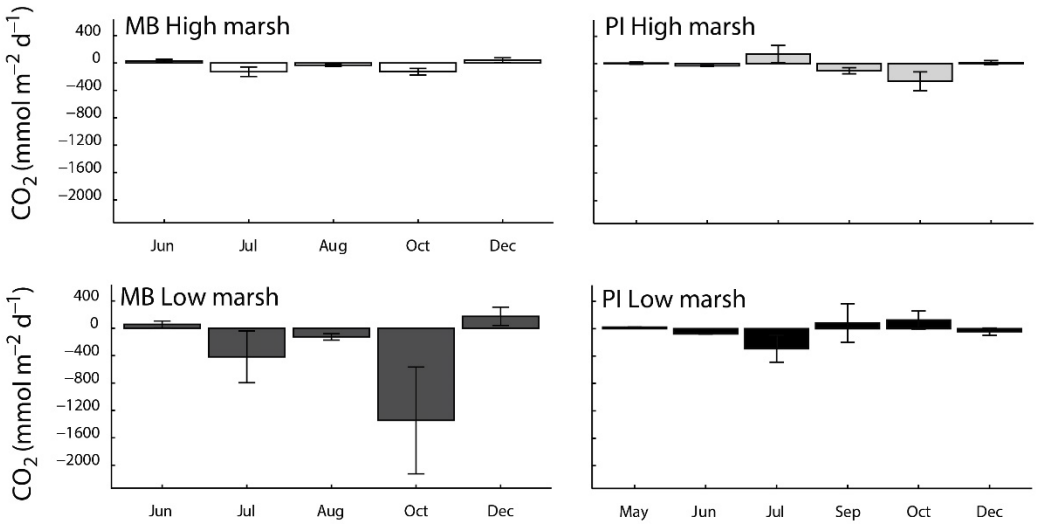


Figure 7. Carbon dioxide fluxes measured at Monie Bay and Poplar Island for each month of sampling split into panels per marsh and vegetation zone. Error bars represent standard error of the mean fluxes. Positive fluxes are out of the sediment.

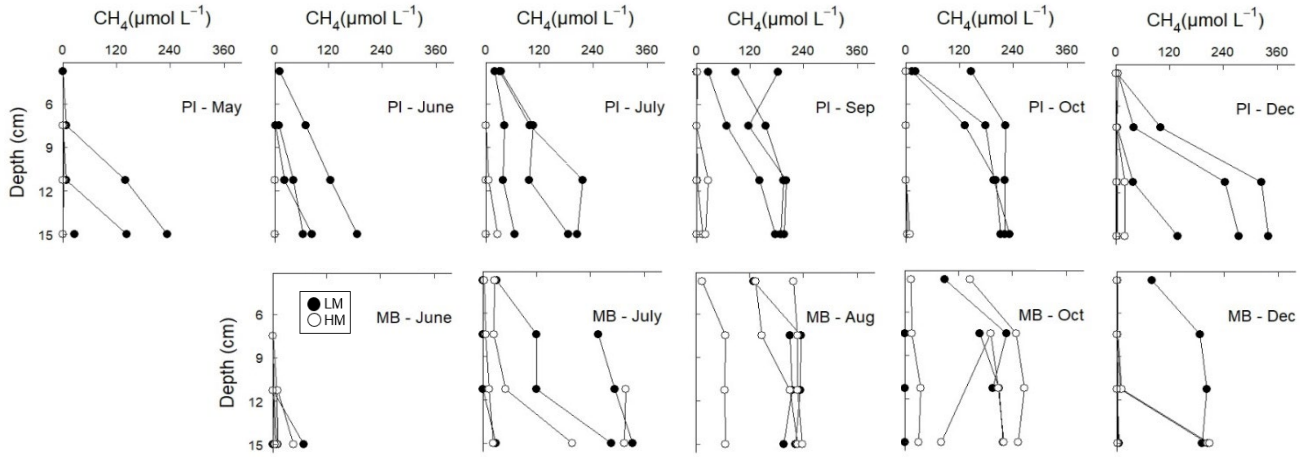


Figure 8. Dissolved methane concentrations in porewater equilibrators in each month of sampling. Missing data occurs where the uppermost sampling wells were dry.

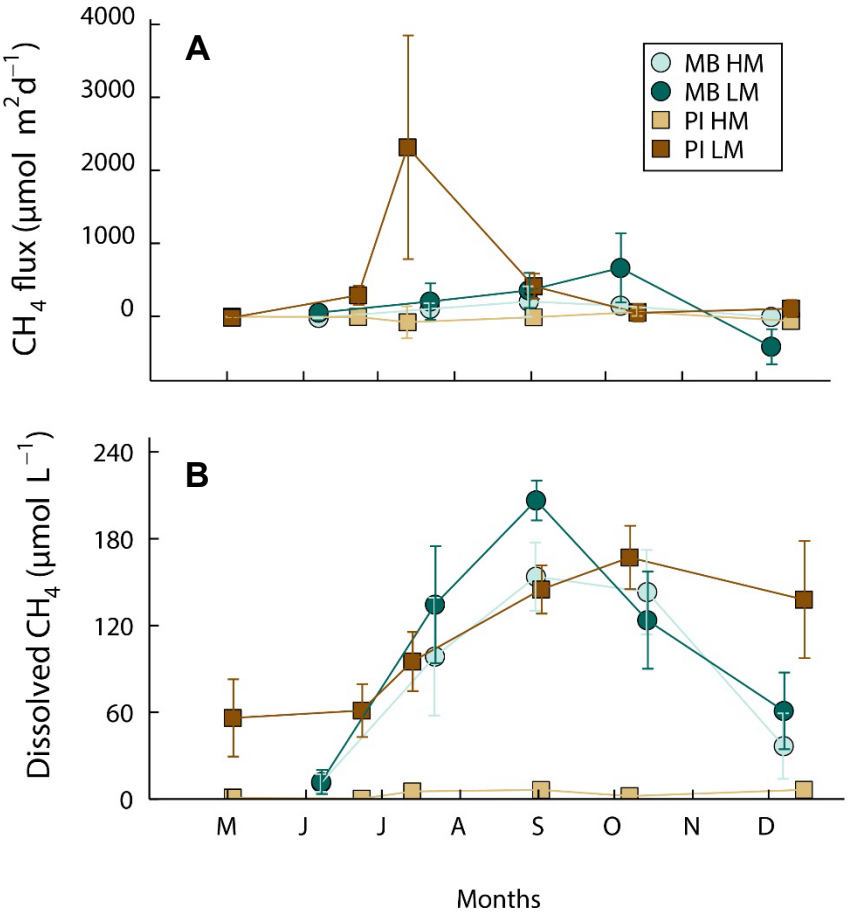


Figure 9. Seasonal methane fluxes in the marshes of Monie Bay and Poplar Island (A). Seasonal concentrations of dissolved methane observed in the porewater equilibrators on each sampling date (B). Error bars represent standard error of the mean.

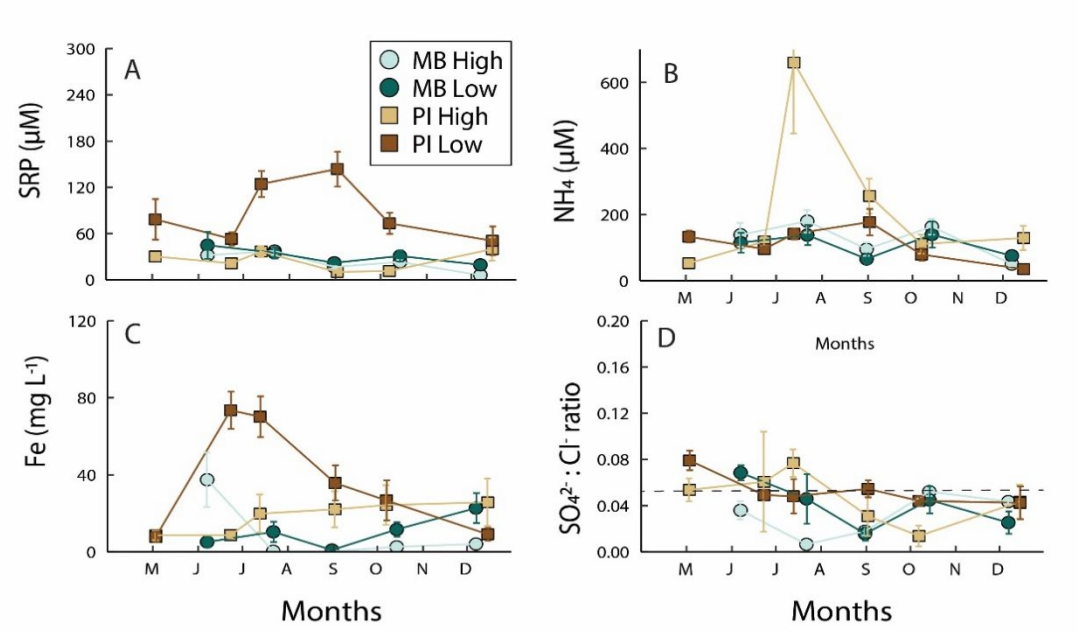


Figure 10. Porewater concentrations of soluble reactive phosphorus (A), ammonium (B), iron (C), and the sulfate to chloride ratio (D) observed in marsh porewater equilibrators through the sampling period. Error bars represent standard error of the mean. Dashed horizontal line in D shows the sulfate to chloride ratio found in seawater, 0.052.

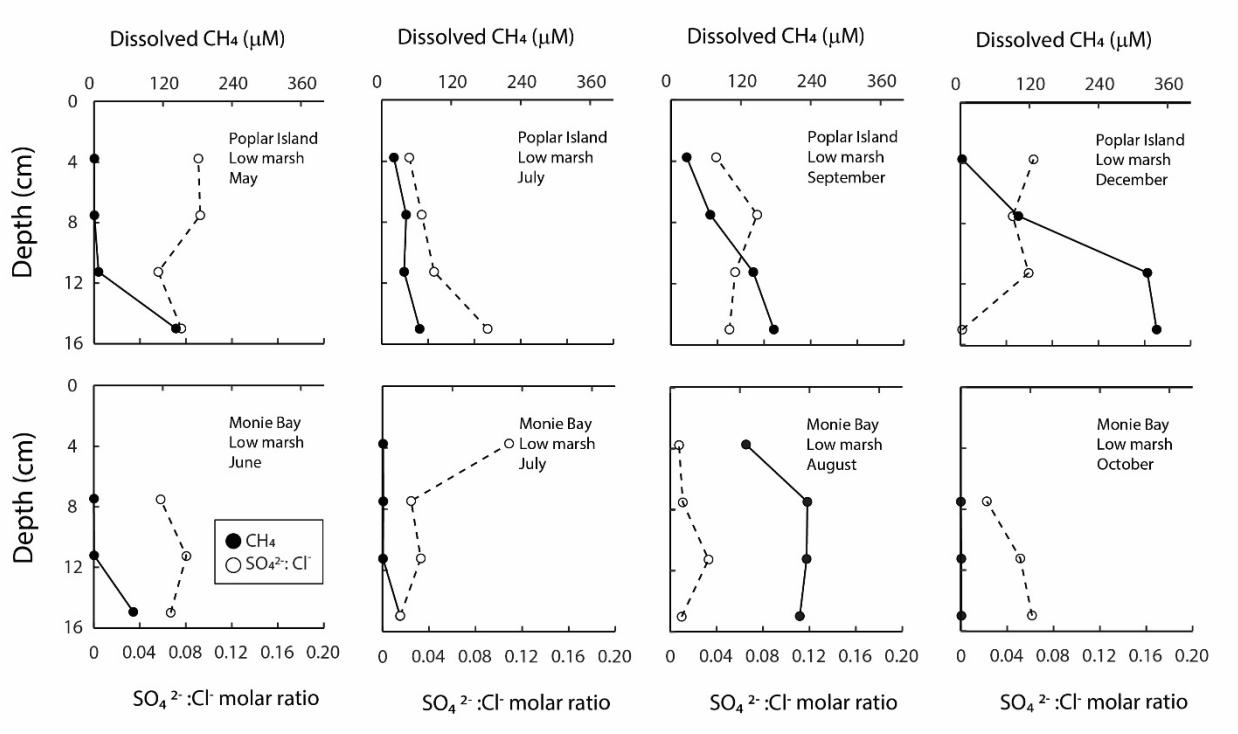


Figure 11. Methane concentration and sulfate to chloride molar ratios in marsh pore waters. Black circles and solid lines $CH_4$, open circles and dashed lines $SO_4$:Cl molar ratio.

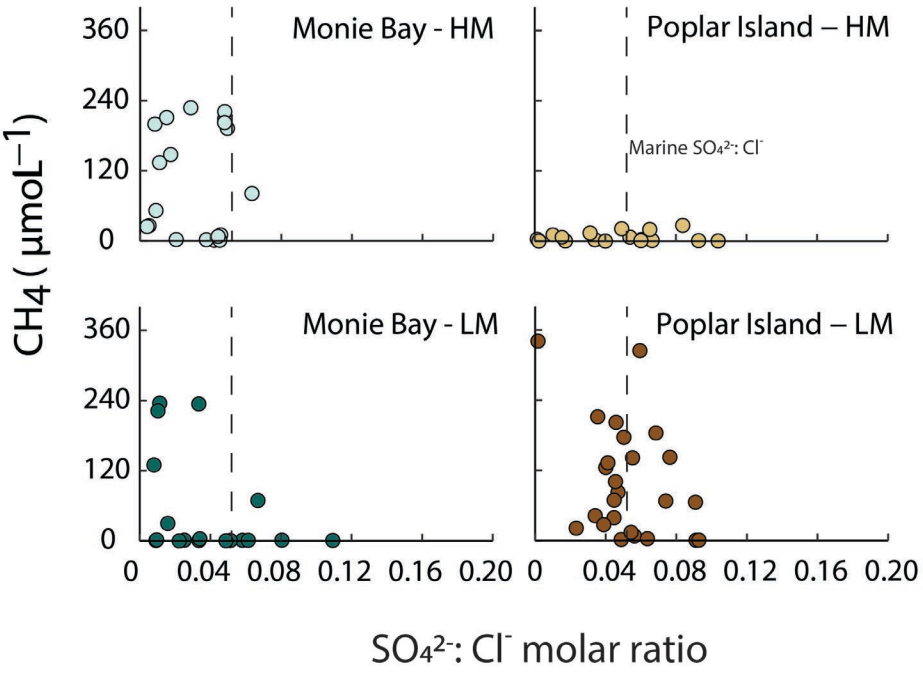


Figure 12. Average $SO_4^{2-}$ : $Cl^-$ molar ratios in the top 15 cm of marsh sediments versus dissolved methane. Dashed line represents expected marine ratio.

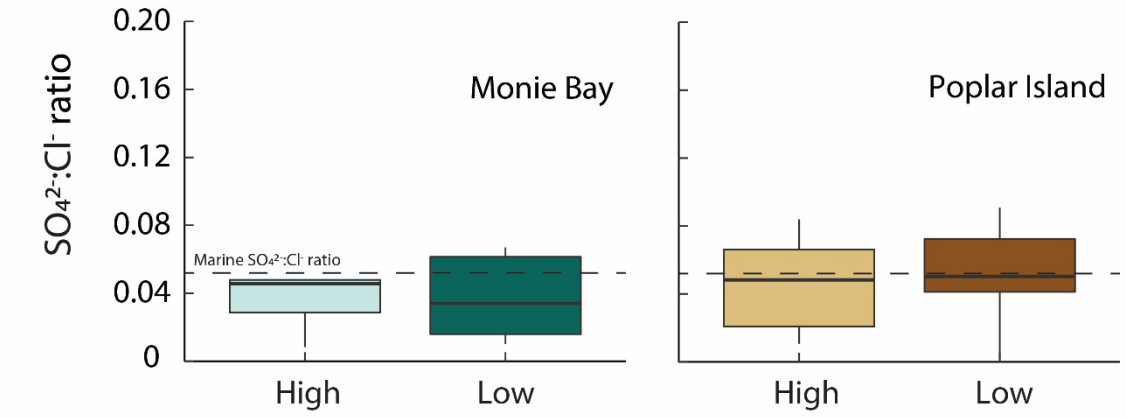


Figure 13. Boxplots of $SO_4^{2-}$ : $Cl^-$ molar ratio at 15cm depth of marsh sediments. Dashed line represents expected marine ratio.

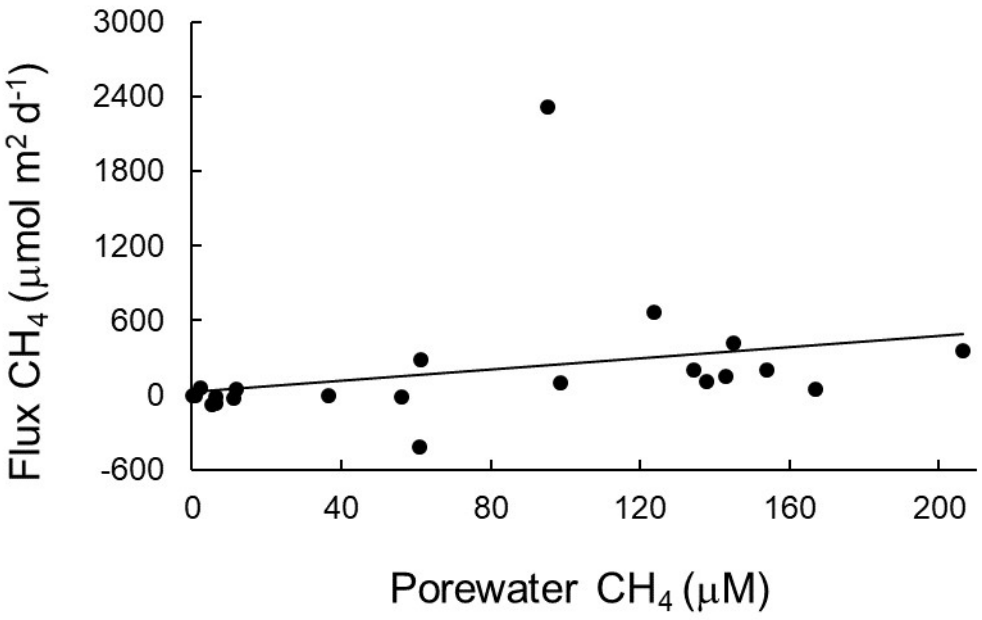


Figure 14. Measured fluxes using static chamber techniques and methane concentrations in sediment porewater.

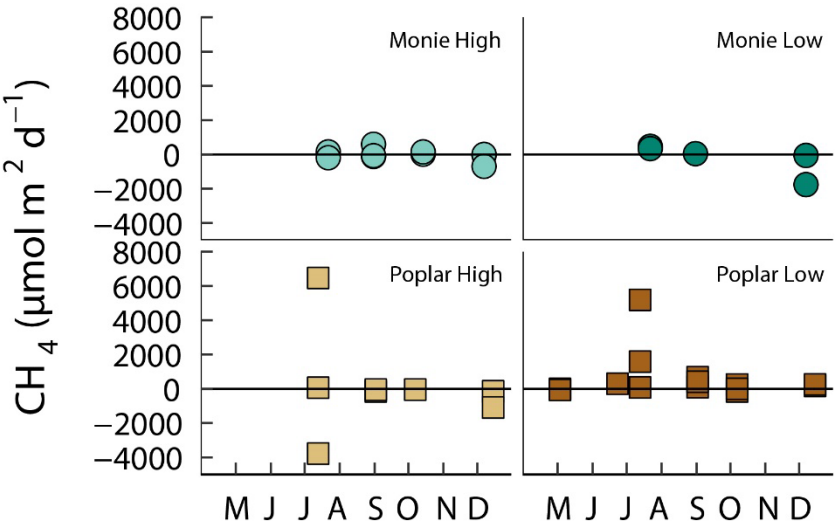


Figure 15. The difference between methane flux rates based on static flux chamber measurements and the flux rates calculated based on diffusion gradients in sediment porewater. The line at 0 represents no difference, positive values indicate observations based on static flux chambers are greater than would be expecting owing to diffusion.

# Appendices

Appendix A: Additional figures.

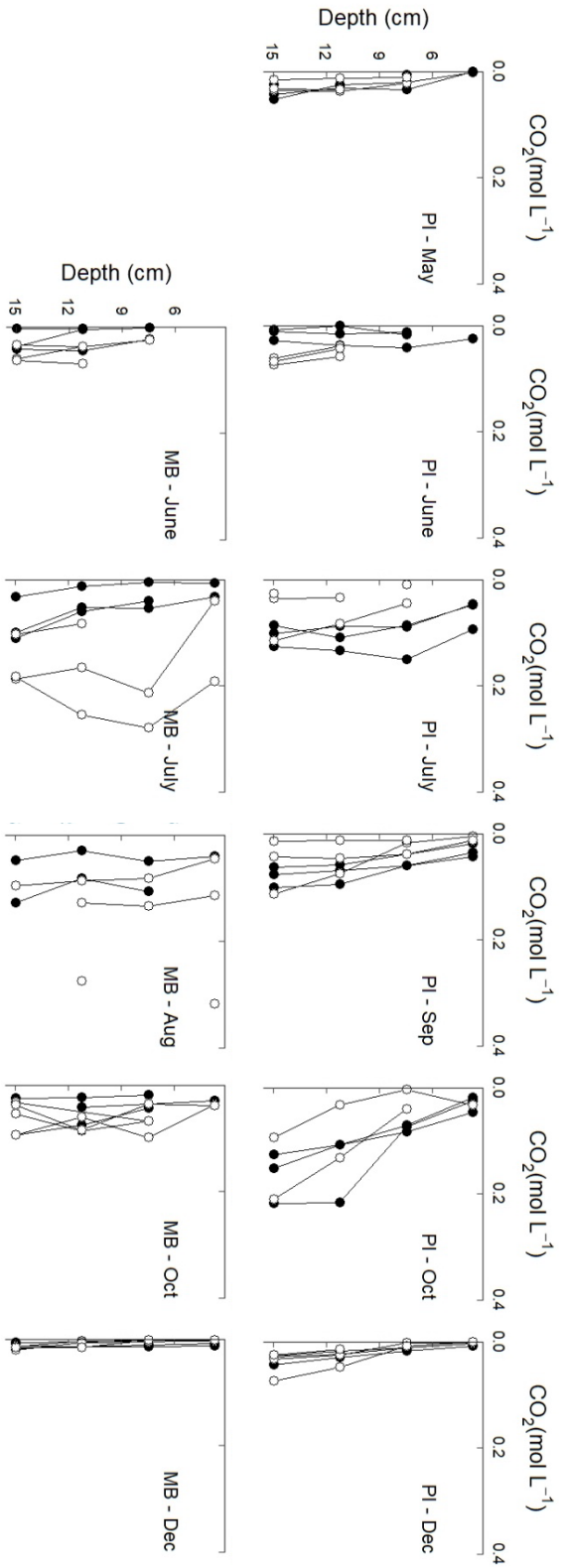


Figure A-1. Dissolved carbon dioxide in marsh porewaters throughout sampling period. Black circles show low marsh samples, white circles show high marsh samples.

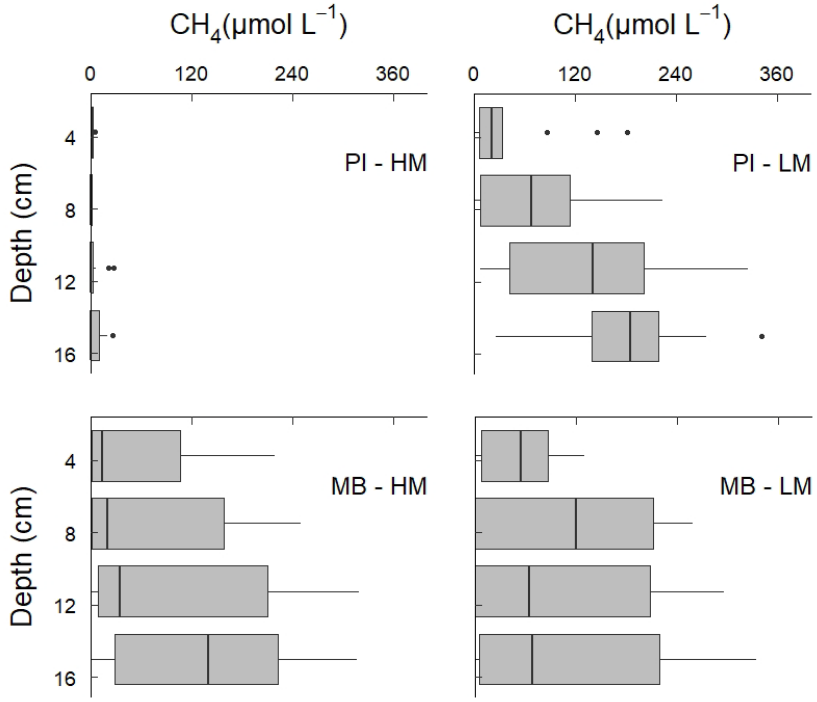


Figure A-2. Boxplots of dissolved methane for all sampling dates. There are between 51 and 71 observations per site.

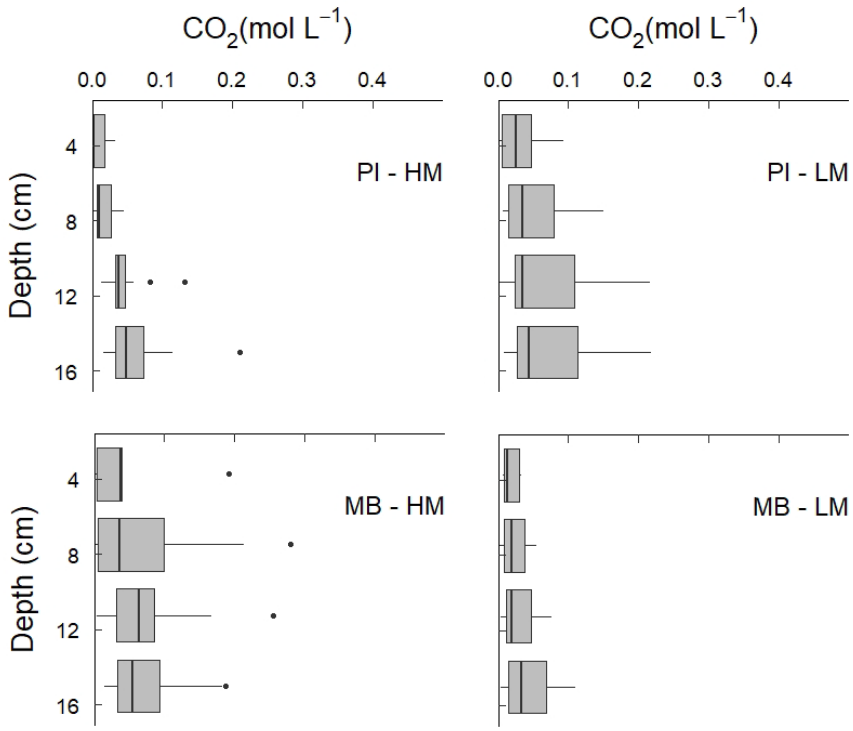


Figure A-3. Boxplots of dissolved carbon dioxide for all sampling dates. There are between 51 and 71 observations per site.

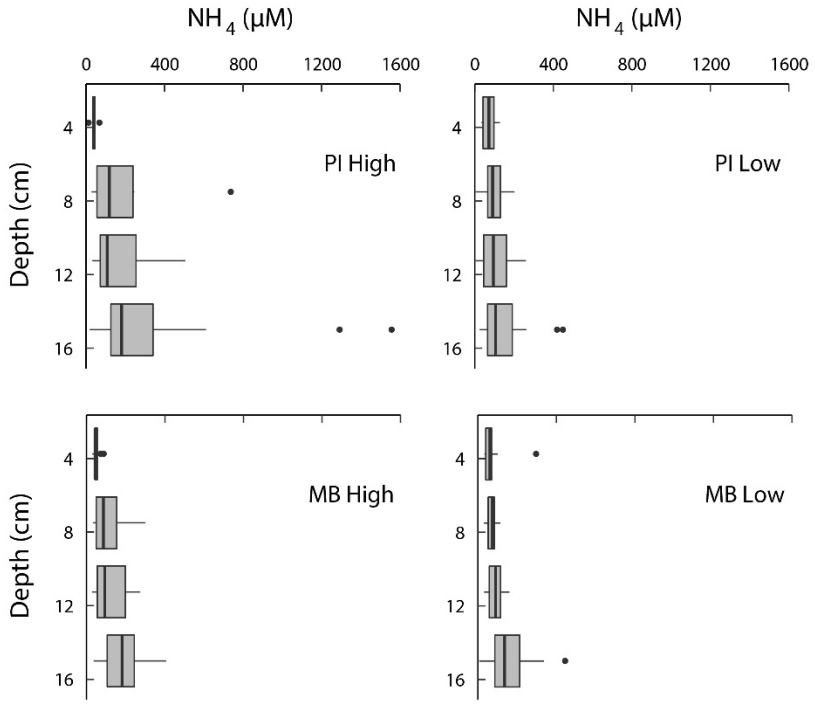


Figure A-4. Boxplots of dissolved ammonium for all sampling dates. There are between 52 and 66 observations per site.

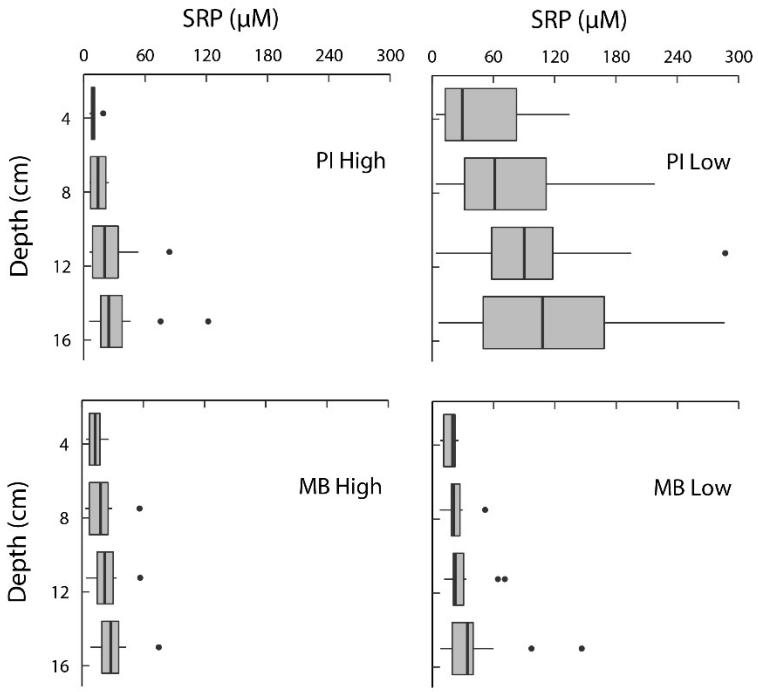


Figure A-5. Boxplots of soluble reactive phosphorus for all sampling dates. There are between 51 and 67 observations per site.

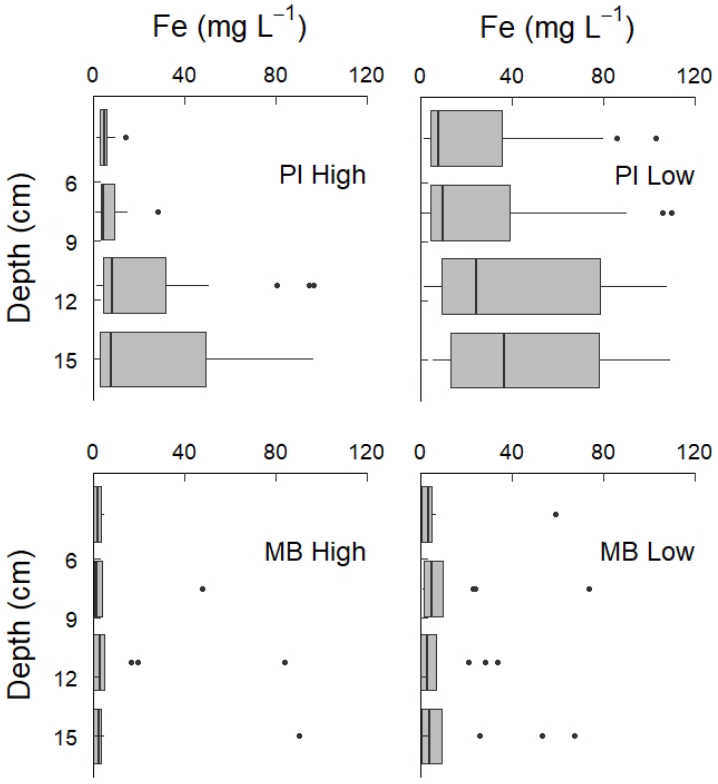


Figure A-6. Boxplots of total iron for all sampling dates. There are between 52 and 67 observations per site.

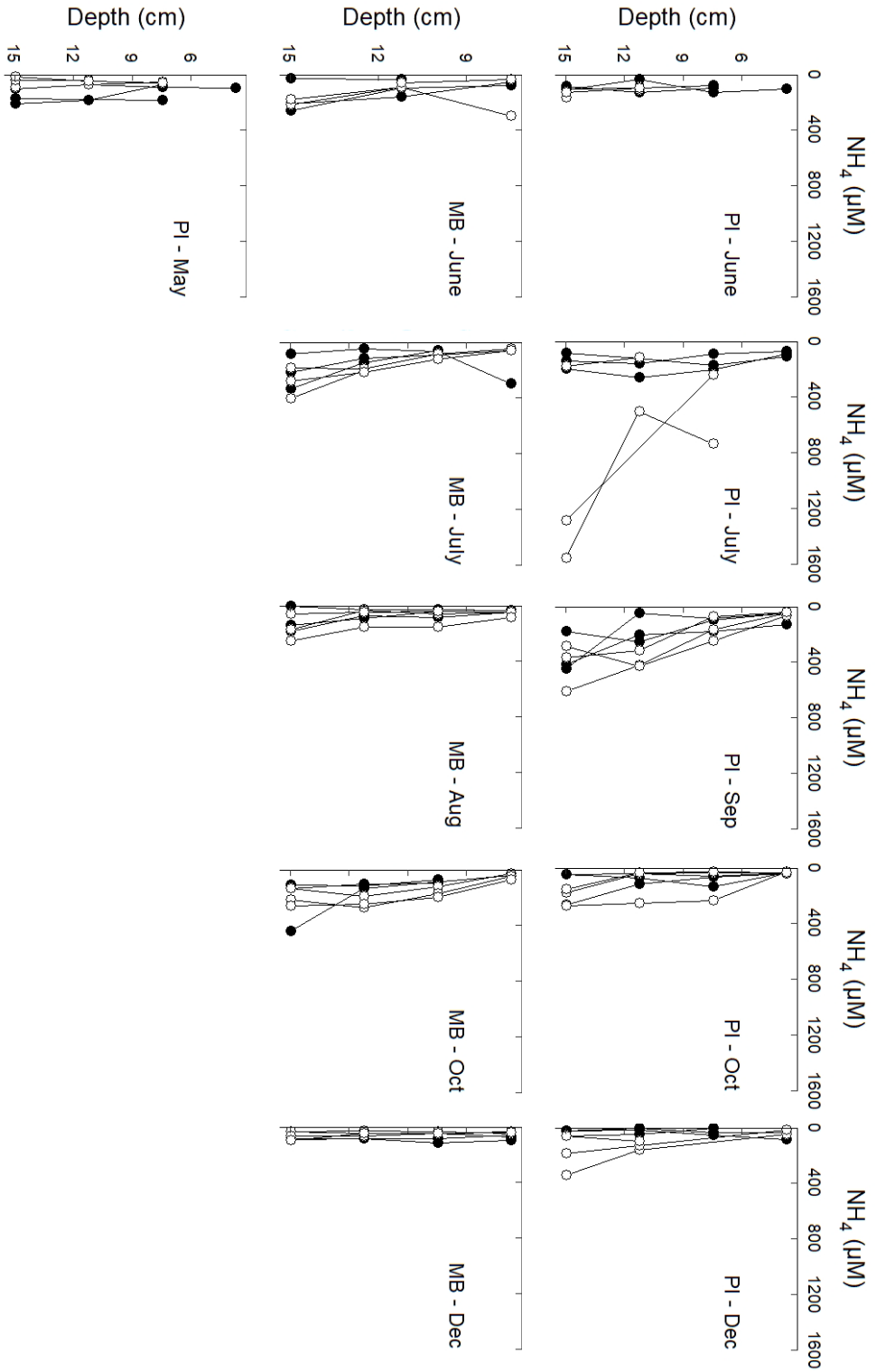


Figure A-7. Dissolved ammonium in marsh porewaters throughout sampling period. Black circles show low marsh samples, white circles show high marsh samples.

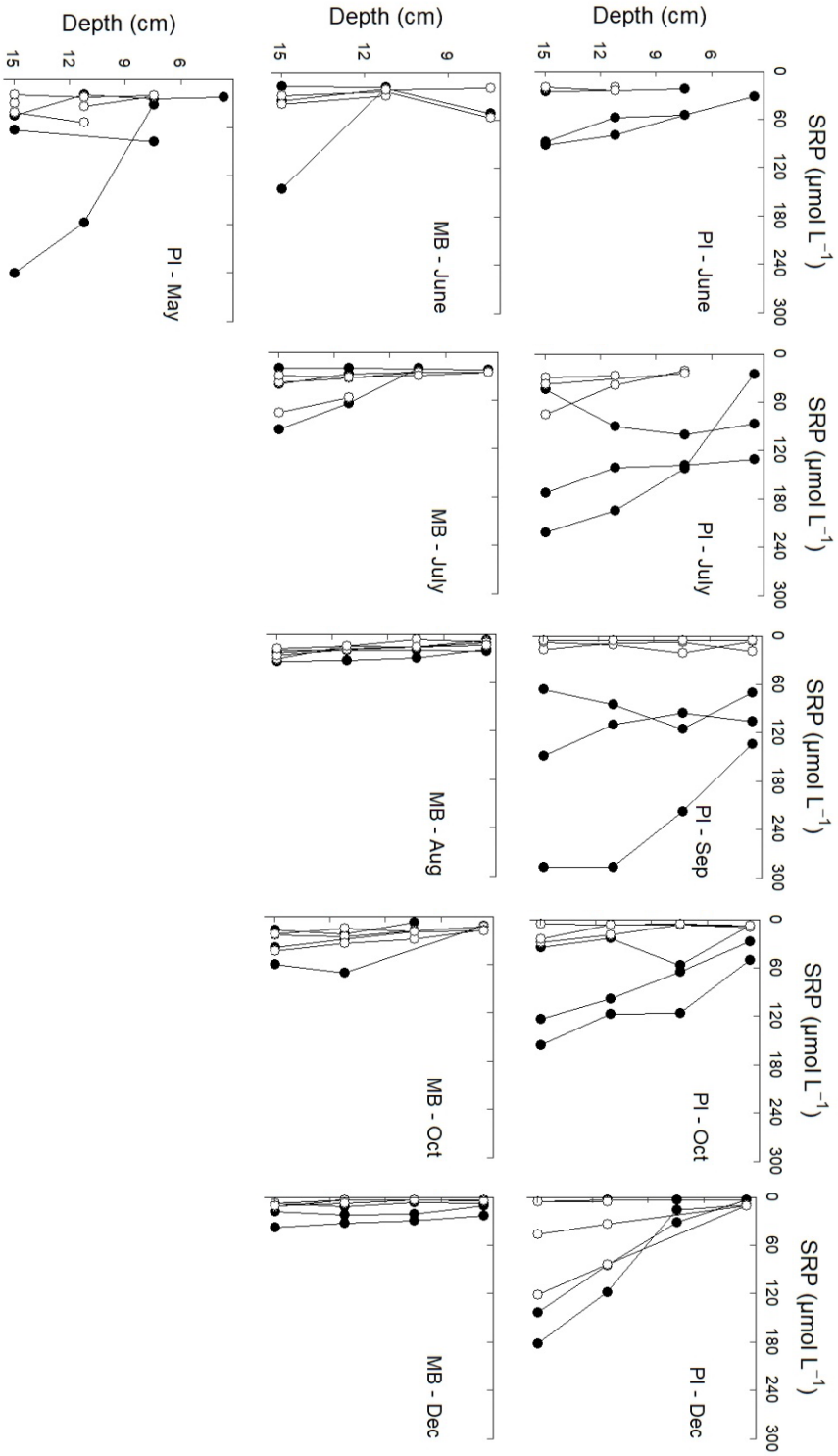


Figure A-8. Soluble reactive phosphorus in marsh porewaters throughout sampling period. Black circles show low marsh samples, white circles show high marsh samples.

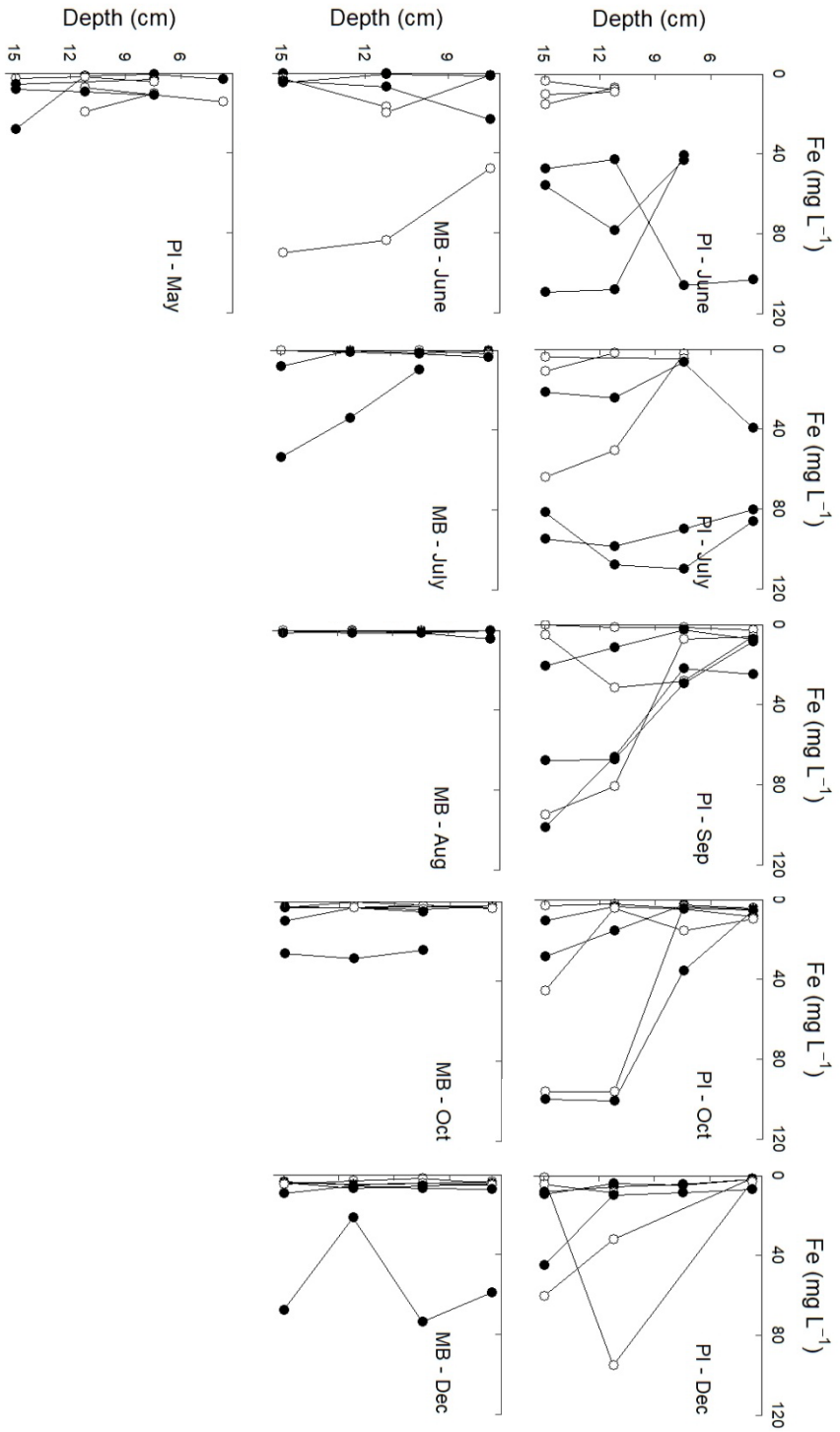


Figure A-9. Iron in marsh porewaters throughout sampling period. Black circles show low marsh samples, white circles show high marsh samples.

Appendix B: Drivers of methane flux from brackish Chesapeake Bay marshes: A mini-review and experiment.

## *Introduction*

Understanding the geochemical and biological drivers of methane production and flux remains a question in wetland ecosystem science. There is interest in the role of plants in regulating fluxes, as well as in quantifying contributions of methane transport pathways, and in identifying methane production mechanisms in these marsh ecosystems. In this appendix, I explore how these factors may be relevant to the methane emissions observed at the study sites described in the body of this thesis.

### *Transport pathways*

Methane is transported from sediments to the atmosphere through three pathways: ebullition (bubbling), diffusion, and plant transport (Chanton and Dacey 1991, Chanton et al. 1992, Chanton et al. 2005, Whalen et al. 2005). In Australia's Cattai Wetland, Jeffrey et al. (2019) partitioned the three sources of methane release and found that plant transport was responsible for upwards of 60% of methane flux. In an arctic wet meadow tundra experiment, Schimel et al. (1995) found plants accounted for an average 75% of methane flux. In rice paddies plant transport was largely responsible for methane emissions observed in those wet agricultural systems (Cicerone and Shetter 1981, Holzapfel-Schorn et al. 1986, Schutz et al. 1989, Nouchi et al. 1990). In a study of reclaimed and pristine wetlands Schipper and Reddy (1994) found that diffusive flux accounted for less than five percent of the plant mediated emissions demonstrating the greater contribution by either ebullition or plant transport. On the other hand, King and Wiebe (1978) and Seyfferth et al. (2020) found ebullition to be an important flux pathway in

studies conducted in salt marshes along the coast of Georgia and Delaware. As a result of these inconsistencies in prominent transport pathways, future research at our study sites is needed to partition the contributions of the three pathways to the observed flux rates. Early workers demonstrated the importance of methane bubble formation as an escape pathway in marine sediments of Chesapeake Bay and Long Island sound by documenting the stripping of dissolved gasses $N_2$ and Ar (Reeburgh 1969, Martens and Berner 1974). I did not measure these gases; however, it is possible that their concentrations in anoxic marsh sediments may similarly be used to understand the importance of bubble formation in methane escape from the marsh. Quantifying methane that is emitted through ebullition, plant transport, or diffusive flux would enable scientists to improve mechanistic models of contemporary methane emissions and also to predict emissions under future climate change scenarios.

*Pathways of methanogenesis*

In addition to determining the pathway by which methane is released, future research at our study sites would benefit from an increased understanding of the mechanism by which it is formed. Anaerobic microbial methane formation is carried out by a diverse community of microorganisms, which has been reviewed in detail by Conrad (2020). Methane production tends to occur through either aceticlastic or hydrogenotrophic pathways in most anoxic environments (Conrad 2020). The former involves the splitting of acetate into $CH_4$ and $CO_2$, whereas the latter consists of the conversion of $H_2$ and $CO_2$ (Conrad 2020). However, methylotrophic methanogenesis has also been identified as a potentially important pathway. Methylotrophic methanogenesis occurs when methyl compounds are converted to $CH_4$ and $CO_2$ (Conrad 2020). Alternatively, methylotrophic formation can lead to $CH_4$ and $H_2O$ when methanol is degraded with $H_2$ (Conrad 2020).

Improving models of global methane emissions hinges on understanding the controls on methane production pathways across aquatic ecosystems. For example, increasing temperatures are expected to yield higher methane emissions by increasing the rate of methane production. However, there may be some nuance based on microbial ecology. For instance, the proportion of hydrogenotrophic methanogenesis has been shown to decline as temperatures decrease, releasing aceticlastic methanogens from competition for substrates and resulting in greater production of methane through acetoclastic pathways (Conrad 2020). We might expect acetclastic methanogens to succeed while hydrogenotrophic methanogen populations decline (Conrad 2020). Therefore, it could be possible that temperature change results in no overall change to emissions if diverse populations of methanogens can succeed under different environmental conditions.

Anthropogenic drivers such as nitrogen loading and concentrations of atmospheric $CO_2$ could also influence the pathways of methane formation as an indirect result of plant physiological change. For example, *S. alterniflora* is expected to exhibit a decrease in the ratio of below ground to above ground biomass when exposed to nitrogen enrichment (Valiela et al. 1976) and elevated $CO_2$ is expected to influence nitrogen uptake kinetics (Cott et al. 2018, Noyce et al. 2019). If climate change or nitrogen availability modify plant biomass or physiology and that subsequently alters the form of available organic material to the marsh microbial community, then one might expect possible changes to methane formation pathways. For example, an increase in the proportion of chitin to cellulose would provide the conditions for an increase in the proportion of aceticlastic to hydrogenotrophic methanogenesis (Conrad 2020). In contrast, an increase in the availability of reduced organic material, such as lipids, may lead to an increase in the importance of hydrogenotrophic methanogenesis (Conrad 2020). Whether the

ratio of above to belowground biomass changes the availability of chitin, cellulose, or lipids in the sediment profile should be explored. Moreover, much of this research is based on theoretical thermodynamic and stoichiometric constraints and there is ample room for study on pathways of methanogenesis in both field and laboratory experiments. How production pathways are shaped by plant-microbe-sediment interactions may be particularly important to understanding responses of marsh ecosystems to global change.

The question as to how sulfate availability controls emissions of methane can also be explored through the lens of methanogen community ecology. Shipper and Reddy (1994) found methane production occurred in the presence of sulfate concentrations up to 20 mg $SO_4^{2-}$, leading them to hypothesize that methanogenic microbes may be active in microsites of soil aggregates or organic particles where sulfate is depleted. Others also disputed the conceptual model of layered anaerobic respiratory activity in favor of a model with multiple pathways cooccurring (Shipper and Reddy 1994 and references therein). More recently, Seyfferth et al. (2020) in their study of salt marshes along the Delaware coast found concentrations of methane below 40 cm depth as high as 892 μM $CH_4$ in the presence of sulfate concentrations of 17 mM in short *Spartina* and 6mM in tall *Spartina.* This led them to hypothesize that across the marsh platform there is heterogeneity in the pathway of methane production with short *Spartina* zones likely exhibiting methylotrophic methanogenesis, while methane production occurred via aceticlastic or hydrogenotrophic methods in tall *Spartina* zones.

A few approaches have been used to explore the competition between microorganisms for substrates and importance of methane formation pathways; these include inhibitor studies and stable isotope analysis. Inhibitors are employed by adding a concentration of a known inhibitor to an incubation containing a target organism with the expectation that it will be effective at

shutting down metabolic activity or a specific process (Oremland and Capone 1988). For example, sodium molybdate is an inhibitor of sulfate reducing bacteria (Oremland and Capone 1988). Oremland and Taylor (1977) were able to show that sulfate reducers were primarily responsible for $H_2$ uptake, outcompeting hydrogenotrophic methanogens for substrates by using sodium molybdate as an inhibitor of sulfate reduction. They also describe endogenous production of methane cooccurring with sulfate reduction, which could be explained by interactions of methanogens with other microbes (Oremland and Taylor 1977). Oremland and Taylor (1977) along with contemporary workers hypothesized one explanation for the increase in methane production under a molybdate treatment was the oxidation of methane by sulfate reducing bacteria.

Inhibitors have also been employed when looking at the use of other competitive substrates. For instance, Kiene (1988) in a study of dimethyl sulfide (DMS) metabolism in salt marsh sediments found sulfate reducers and methanogens were both utilizing DMS. Both molybdate and 2-bromoethanesulphonic acid (BES) blocked consumption of DMS, with molybdate yielding increased inhibition. Kiene (1988) hypothesized that DMS may contribute minimally to total sulfate reduction, while playing a dominant role in methane production in salt marsh soils, contributing only 1% to overall rates of sulfate reduction yet 28% to total methane production. The addition of methanol, trimethylamine (TMA), and methionine have also been explored as potential competitive substrates between sulfate reducers and methanogens (Oremland and Polcin 1983). Oremland and Polcin (1983) found that while sulfate reducers outcompete methanogens for hydrogen and acetate, the same was not observed for methanol, TMA, or methionine. Moreover, Oremland et al. (1982) show that when the methanogen inhibitor BES was added to flasks of a sediment slurry from the salt marsh of San Francisco

Bay, methane production was inhibited and the pool of TMA and methanol increased with time indicating the importance of these non-competitive substrates. This provided early evidence that methanogenesis and sulfate reduction could cooccur in sulfate-rich marine sediments provided alternative non-competitive substrates were available. It is possible that plant material plays a role in the non-competitive substrate metabolism. King (1983) found TMA accounted for a low proportion of methane produced from sediment incubations from the rockweed (*Ascophyllum nodosum*) covered sediments of Lowes Cove, Maine, in contrast to TMA accounting for 90% of methane production in sediments from a San Francisco Bay salt marsh amended with *Spartina foliosa.* Methylated amines are abundant in halophytes, such as *Spartina* spp., and may thus provide for a larger supply of the methane produced in marsh ecosystems (King 1983). And, as was noted by Krause and Treude (2021), methanol is formed during the degradation of pectin and lignin in plant cell walls (Krause and Treude 2021, Schink and Zeikus 1980, Donnelly and Dagely 1980). Lignocellulose comprises the bulk of anatomical structures in *S. alterniflora* (Hodson et al. 1984).

Another consideration is that the incoming tide is also a source of dissolved organic carbon (DOC) to the salt marsh, providing energy for microbial activity (Hemminga 1993 *in* Seyfferth 2020). Because DOC often acts as the rate limiting step in microbial respiration (Seyfferth and references therein), a relevant question is how much methane produced in the marsh originates from carbon provided by allochthonous DOC in tidewater? And, if methanogenesis proceeds through methylotrophic pathways, then does the autochthonous DOC pool exert greater control when the release of methylamines is reliant on the degradation of *Spartina* sp. (Seyfferth 2020). Whether methylamines are supplied externally or produced internally may have important implications for methane production in these systems.

I conducted a preliminary experiment to understand how the competition between sulfate reduction and methanogenesis plays out in the marshes of Poplar Island using sodium molybdate to inhibit sulfate reduction.

***Methods***

Twelve sediment cores were collected on two separate sampling dates in July and August 2021 from the marsh at Poplar Island. Cores were taken from areas where an algal covering occurred on the marsh surface and bubbles were observed (Fig B-1). Samples were collected with clear acrylic plastic tubes (15cm height, 3.75 cm inner diameter) and capped with a gas-tight clear acrylic lid and bottom stopper that has a rubber septum injection port for sampling the gas headspace.

Four sediment cores received a treatment of Choptank River water (salinity 10), four cores received a treatment of DI water, and to the remaining four was added a solution of 10mM sodium molybdate to approximately match the concentration of sulfate in the Choptank River (Figure B-2). Cores were kept under a UV light, to mirror diel cycles, and light and dark measurements of headspace $CH_4$ concentration were made. The headspace of each core was sampled by extracting 0.5 mL using a gas-tight syringe. The sample was immediately injected into a Shimadzu gas chromatograph with a flame ionization detector for analysis.

***Results***

Across all treatments and sampling dates, the greatest methane production observed occurred in the sodium molybdate amended cores (Fig B-3). There were no significant differences amongst treatments at any time point throughout the experiment.

***Discussion***

Based on the inhibitor experiments described in the above section, a few explanations for

the results emerge. The first is that sulfate reduction does inhibit methanogenesis in the marshes of Poplar Island, and our mixed results were a consequence of incubation design, length, or sediment core heterogeneity (some cores visually show high sulfide build-up whereas others have signs of bioturbation and oxygenation, figure SI 12). Or there could have also been within core heterogeneity with simultaneous sulfate reduction and methanogenesis. The second is that methylotrophic methanogenesis plays some role at our site and the inhibition of sulfate reduction by molybdate and subsequent alleviation from competition of acetate and hydrogen did not immediately lead to methane production. However, these results are preliminary and should be followed up on.

Stable isotope analysis is another strategy to document the different pathways of methanogenesis. In the oceanic sulfate-to- methane transition zone, workers used the stable isotope values of $\delta^{13}C$ to determine whether in-situ methane production occurs in the sulfate zone (Kessler 2008). Deeper methane profiles had more negative $\delta^{13}C$ than those within the shallower sulfate zone (Kessler 2008). Zhuang et al. (2018) used this strategy in studying Mediterranean delta and shelf sediments and found methylotrophic methanogenesis dominated at the shelf site, whereas the delta site had high rates of aceticlastic and hydrogenotrophic methanogenesis. They speculated that this could be due to the composition of the organic carbon pool, with coastal waters of the delta delivering abundant labile organic matter to those sediments (Zhang et al. 2018) . Considering this finding in the context of the salt marsh system, it could be that there also exist differences in methane formation pathways through depth in marsh sediments depending on the organic carbon pool, as was hinted at by Seyfferth et al. (2020).

In support of this hypothesis, Buckley et al. (2008) found a vertical gradient of methane

metabolism in soft microbial mats in Great Sippewissett Marsh with the methanogen community below the chemocline (10-50mm) appearing to consist primarily of obligately methylotrophic methanogens unable to use $H_2$ or acetate. In that same study, inhibition of sulfate reducers did lead to the enrichment of hydrogenotrophic methanogens at these depths suggesting stains of microbes capable of growth on $H_2$ were present. Interestingly, in the upper 0-5mm of the microbial mat at Great Sippewissett, the cyanobacterial layer, these workers found the simultaneous addition of molybdate and hydrogen suppressed methanogen growth demonstrating that methanogens may benefit from sulfate reducers consuming $H_2$ before its accumulation inhibits fermentative processes that allow for the production of metabolically usable carbon sources (Buckley et al. 2008). Those workers suggest the activity of the methylotrophic methanogen *Methanosphaera*, capable of growing on methanol and $H_2$, but unable to use $CO_2$ or TMA as a carbon source (Buckley et al. 2008). In China's Yancheng National Nature Reserve, sediment incubations from marshes invaded with *Spartina alterniflora* showed a greater response to the addition of TMA than to acetate or hydrogen and the methylotrophic methanogen *Methanosarcinacae* became the dominant methanogen (Yuan et al. 2016). Ongoing work by other students and researchers at Poplar Island seeks to characterize the microbial ecology of this marsh system.

***Conclusions***

Future work to understand the dynamics of methane production at our site should link microbial community ecology with rate measurements of methane production and inhibitor experiments on incubations of methanogens, methanotrophs, and sulfate reducers to characterize the primary substrates limiting methanogenesis at this site.

Figure B-1. Photo of marsh surface where sediment cores were retrieved from Poplar Island in July and August 2021 for the core incubation experiment.


Figure B-2. (A) Sediment core post-incubation with DI treatment, note black areas representing sulfidic layers. (B) Sediment core post-incubation with Choptank River water, note reddish area indicating oxygenation. (C) Sediment core samples for August 2021 trial – note lack of uniformity across cores. (D) Sediment core samples for July 2021 trial – note lack of uniformity across cores.

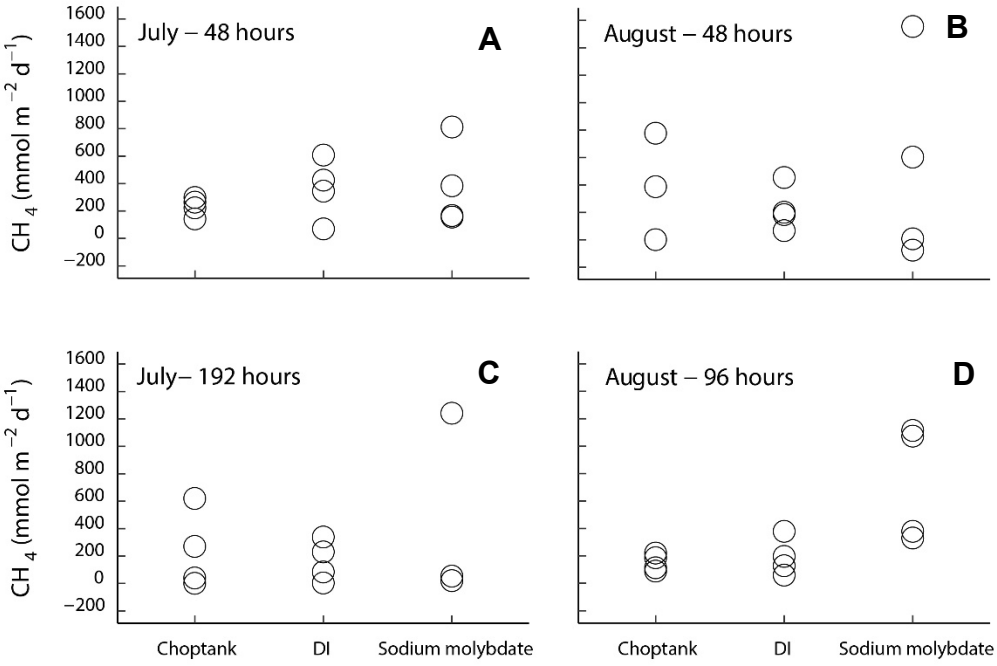


Figure B-3. Methane production in sediment core incubations treated with Choptank River water, DI water, and Sodium molybdate after 48 hours of treatment in July (A), 192 hours of treatment in July (B), 48 hours of treatment in August (C), and 96 hours of treatment in August (D).

# Bibliography

Abbott, K. M., T. Elsey-Quirk, and R. D. DeLaune. 2019. Factors influencing blue carbon accumulation across a 32-year chronosequence of created coastal marshes. *Ecosphere* 10.

Abril, G., and N. Iversen. 2002. Methane dynamics in a shallow non-tidal estuary (Randers Fjord, Denmark). *Marine Ecology Progress Series* 230: 171–181.

Altor, A. E., and W. J. Mitsch. 2006. Methane flux from created riparian marshes: Relationship to intermittent versus continuous inundation and emergent macrophytes. *Ecological Engineering* 28: 224–234.

Apple, J. K., P. A. del Giorgio, and R. I. E. Newell. 2004. The Effects of System-Level Nutrient Enrichment on Bacterioplankton Production in a Tidally-Influenced Estuary. *Journal of Coastal Research*: 110–133.

Ardón, M., A. M. Helton, and E. S. Bernhardt. 2018. Salinity effects on greenhouse gas emissions from wetland soils are contingent upon hydrologic setting: a microcosm experiment. *Biogeochemistry* 140: 217–232.

Arias-Ortiz, A., P. Y. Oikawa, J. Carlin, P. Masqué, J. Shahan, S. Kanneg, A. Paytan, and D. D. Baldocchi. 2021. Tidal and Nontidal Marsh Restoration: A Trade-Off Between Carbon Sequestration, Methane Emissions, and Soil Accretion. *Journal of Geophysical Research: Biogeosciences* 126.

Baldwin, A. H., P. J. K. Angas, J. P. Megonigal, M. T. C. Perry, and D. F. Whigham. Coastal Wetlands of Chesapeake Bay: 16.

Bartlett, K. B., D. S. Bartlett, R. C. Harriss, and D. I. Sebacher. 1987. Methane emissions along a salt marsh salinity gradient. *Biogeochemistry* 4: 183–202.

Bartlett, K. B., and R. C. Harriss. 1993. Review and assessment of methane emissions from wetlands. *Chemosphere* 26: 261–320.

Bridgham, S. D., H. Cadillo-Quiroz, J. K. Keller, and Q. Zhuang. 2013. Methane emissions from wetlands: biogeochemical, microbial, and modeling perspectives from local to global scales. *Global Change Biology* 19: 1325–1346.

Bridgham, S. D., J. P. Megonigal, J. K. Keller, N. B. Bliss, and C. Trettin. 2006. The carbon balance of North American wetlands. *Wetlands* 26: 889–916.

Buckley, D. H., L. K. Baumgartner, and P. T. Visscher. 2008. Vertical distribution of methane metabolism in microbial mats of the Great Sippewissett Salt Marsh. *Environmental Microbiology* 10: 967–977.

Chanton, J. P. 2005. The effect of gas transport on the isotope signature of methane in wetlands. *Organic Geochemistry* 36: 753–768.

Chanton, J. P., and J. W. H. Dacey. 1991. Effects of Vegetation on Methane Flux, Reservoirs, and Carbon Isotopic Composition. In *Trace Gas Emissions by Plants,* eds. Sharkey, Holland, Mooney, 65–92. San Diego, CA: Academic Press, Inc.

Chanton, J. P., G. J. Whiting, W. J. Showers, and P. M. Crill. 1992. Methane flux from Peltandra virginica: stable isotope tracing and chamber effects. *Global Biogeochemical Cycles* 6: 15–31.

Chesapeake Bay Program. 2022. Wetlands. https://www.chesapeakebay.net/state/wetlands. Accessed 30 August 2022.

Chmura, G. L., S. C. Anisfeld, D. R. Cahoon, and J. C. Lynch. 2003. Global carbon sequestration in tidal, saline wetland soils. *Global Biogeochemical Cycles* 17.

Chmura, G. L., L. Kellman, L. van Ardenne, and G. R. Guntenspergen. 2016. Greenhouse Gas Fluxes from Salt Marshes Exposed to Chronic Nutrient Enrichment. *PLOS ONE* 11.

Cicerone, R. J., and J. D. Shetter. 1981. Sources of atmospheric methane: Measurements in rice paddies and a discussion. *Journal of Geophysical Research: Oceans* 86: 7203–7209.

Conrad, R. 2020. Importance of hydrogenotrophic, aceticlastic and methylotrophic methanogenesis for methane production in terrestrial, aquatic and other anoxic environments: A mini review. *Pedosphere* 30: 25–39.

Cornell, J. A., C. B. Craft, and J. P. Megonigal. 2007. Ecosystem gas exchange across a created salt marsh chronosequence. *Wetlands* 27: 240–250

Cornwell, J. C., M. S. Owens, L. W. Staver, and J. C. Stevenson. 2020. Tidal Marsh Restoration at Poplar Island I: Transformation of Estuarine Sediments into Marsh Soils. *Wetlands* 40: 1673-1686.

Cornwell, J., J. Stribling, and J. Stevenson. 1994. Biogeochemical studies at the Monie Bay National Estuarine Research Reserve. Final Report, National Oceanic and Atmospheric Administration National Estuarine Research Reserve System. Report No. NA89AA/D C2 130, Washington, DC.

Cott, G. M., J. S. Caplan, and T. J. Mozdzer. 2018. Nitrogen uptake kinetics and saltmarsh plant responses to global change. *Scientific Reports* 8.

Craft, C., P. Megonigal, S. Broome, J. Stevenson, R. Freese, J. Cornell, L. Zheng, and J. Sacco. 2003. The pace of ecosystem development of constructed Spartina alterniflora marshes. *Ecological Applications* 13: 1417–1432.

Crill, P. M., and C. S. Martens. 1983. Spatial and temporal fluctuations of methane production in anoxic coastal marine sediments. *Limnology and Oceanography* 28: 1117–1130.

Dacey, J. W. H., and M. J. Klug. 1979. Methane Efflux from Lake Sediments Through Water Lilies. *Science* 203. American Association for the Advancement of Science: 1253–1255.

DeLaune, R. D., C. J. Smith, and W. H. PATRICK Jr. 1983. Methane release from Gulf coast wetlands. *Tellus B* 35B: 8–15.

Derby, R. K., B. A. Needelman, A. A. Roden, and J. P. Megonigal. 2022. Vegetation and hydrology stratification as proxies to estimate methane emission from tidal marshes. *Biogeochemistry* 157: 227–243.

Donnelly, M. I., and S. Dagley. 1980. Production of methanol from aromatic acids by Pseudomonas putida. *Journal of Bacteriology* 142: 916–924.

Gibbs, M. M. 1979. A simple method for the rapid determination of iron in natural waters. *Water Research* 13: 295–297.

Grossart, H.-P., K. Frindte, C. Dziallas, W. Eckert, and K. W. Tang. 2011. Microbial methane production in oxygenated water column of an oligotrophic lake. *Proceedings of the National Academy of Sciences* 108: 19657–19661.

Hemes, K. S., S. D. Chamberlain, E. Eichelmann, T. Anthony, A. Valach, K. Kasak, D. Szutu, J. Verfaillie, W. L. Silver, and D. D. Baldocchi. 2019. Assessing the carbon and climate benefit of restoring degraded agricultural peat soils to managed wetlands. *Agricultural and Forest Meteorology* 268: 202–214.

Hemminga, M. A., V. A. Klap, J. van Soelen, and J. J. Boon. 1993. Effect of salt marsh inundation on estuarine particulate organic matter characteristics. *Marine Ecology Progress Series* 99: 153–161.

Hesslein, R. H. 1976. An in situ sampler for close interval pore water studies1. *Limnology and Oceanography* 21: 912–914.

Hodson, R. E., R. R. Christian, and A. E. Maccubbin. 1984. Lignocellulose and lignin in the salt marsh grass Spartina alterniflora: initial concentrations and short-term, post-depositional changes in detrital matter. *Marine Biology* 81: 1–7.

Holm, G. O., B. C. Perez, D. E. McWhorter, K. W. Krauss, D. J. Johnson, R. C. Raynie, and C. J. Killebrew. 2016. Ecosystem Level Methane Fluxes from Tidal Freshwater and Brackish Marshes of the Mississippi River Delta: Implications for Coastal Wetland Carbon Projects. *Wetlands* 36: 401–413.

Holzapfel-Pschorn, A., and W. Seiler. 1986. Methane emission during a cultivation period from an Italian rice paddy. *Journal of Geophysical Research: Atmospheres* 91: 11803–11814.

Howes, B. L., J. W. H. Dacey, and J. M. Teal. 1985. Annual Carbon Mineralization and Belowground Production of Spartina Alterniflora in a New England Salt Marsh. *Ecology* 66: 595–605.

Jeffrey, L. C., D. T. Maher, S. G. Johnston, B. P. Kelaher, A. Steven, and D. R. Tait. 2019. Wetland methane emissions dominated by plant-mediated fluxes: Contrasting emissions pathways and seasons within a shallow freshwater subtropical wetland. *Limnology and Oceanography* 64: 1895–1912.

Kearney, M. S., J. C. Stevenson, and L. G. Ward. 1994. Spatial and Temporal Changes in Marsh Vertical Accretion Rates at Monie Bay: Implications for Sea-Level Rise. *Journal of Coastal Research* 10: 1010–1020.

Keller, J. K., A. E. Sutton-Grier, A. L. Bullock, and J. P. Megonigal. 2013. Anaerobic Metabolism in Tidal Freshwater Wetlands: I. Plant Removal Effects on Iron Reduction and Methanogenesis. *Estuaries and Coasts* 36: 457–470.

Kelley, C. A., C. S. Martens, and W. Ussler III. 1995. Methane dynamics across a tidally flooded riverbank margin. *Limnology and Oceanography* 40: 1112–1129.

Kessler, J. D., W. S. Reeburgh, D. L. Valentine, F. S. Kinnaman, E. T. Peltzer, P. G. Brewer, J. Southon, and S. C. Tyler. 2008. A survey of methane isotope abundance (14C, 13C, 2H) from five nearshore marine basins that reveals unusual radiocarbon levels in subsurface waters. *Journal of Geophysical Research: Oceans* 113.

Kiene, R. P. 1988. Dimethyl sulfide metabolism in salt marsh sediments. *FEMS Microbiology Ecology* 4: 71–78.

King, G. M., M. J. Klug, and D. R. Lovley. 1983. Metabolism of acetate, methanol, and methylated amines in intertidal sediments of lowes cove, maine. *Applied and Environmental Microbiology* 45: 1848–1853.

King, G. M., and W. J. Wiebe. 1978. Methane release from soils of a Georgia salt marsh. *Geochimica et Cosmochimica Acta* 42: 343–348.

King, Gary M., and W. J. Wiebe. 1980. Regulation of sulfate concentrations and methanogenesis in salt marsh soils. *Estuarine and Coastal Marine Science* 10: 215–223.

Krause, S. J. E., and T. Treude. 2021. Deciphering cryptic methane cycling: Coupling of methylotrophic methanogenesis and anaerobic oxidation of methane in hypersaline coastal wetland sediment. *Geochimica et Cosmochimica Acta* 302: 160–174.

Kroeger, K. D., S. Crooks, S. Moseman-Valtierra, and J. Tang. 2017. Restoring tides to reduce methane emissions in impounded wetlands: A new and potent Blue Carbon climate change intervention. *Scientific Reports* 7.

Lan, X., E. G. Nisbet, E. J. Dlugokencky, and S. E. Michel. 2021. What do we know about the global methane budget? Results from four decades of atmospheric $CH_4$ observations and the way forward. *Philosophical Transactions of the Royal Society A: Mathematical, Physical and Engineering Sciences* 379.

Li, X., and W. J. Mitsch. 2016. Methane emissions from created and restored freshwater and brackish marshes in southwest Florida, USA. *Ecological Engineering* 91: 529–536.

Liu, L.-Y., G.-J. Xie, J. Ding, B.-F. Liu, D.-F. Xing, N.-Q. Ren, and Q. Wang. 2022. Microbial methane emissions from the non-methanogenesis processes: A critical review. *Science of The Total Environment* 806.

Macreadie, P. I., A. Anton, J. A. Raven, N. Beaumont, R. M. Connolly, D. A. Friess, J. J. Kelleway, et al. 2019. The future of Blue Carbon science. *Nature Communications* 10.

Martens, C. S., and R. A. Berner. 1974. Methane production in the interstitial waters of sulfate-depleted marine sediments. *Science* 185: 1167–1169.

Maryland Department of Natural Resources. 2022. Eyes on the Bay: Your home for Maryland tidal water quality data, downloads and visualizations. 2022. *Eyes on the Bay*. Accessed 30 August 2022.

Mcleod, E., G. L. Chmura, S. Bouillon, R. Salm, M. Björk, C. M. Duarte, C. E. Lovelock, W. H. Schlesinger, and B. R. Silliman. 2011. A blueprint for blue carbon: toward an improved understanding of the role of vegetated coastal habitats in sequestering CO2. *Frontiers in Ecology and the Environment* 9: 552–560.

Megonigal, J. P., and W. H. Schlesinger. 1997. Enhanced CH4 emissions from a wetland soil exposed to Elevated CO2. *Biogeochemistry* 37, 77-88.

Merrill, J.Z. 1999. Tidal freshwater marshes as nutrient sinks. Doctoral Dissertation, University of Maryland.

Mostovaya, A., M. Wind-Hansen, P. Rousteau, L. A. Bristow, and B. Thamdrup. 2022. Sulfate- and iron-dependent anaerobic methane oxidation occurring side-by-side in freshwater lake sediment. *Limnology and Oceanography* 67: 231–246.

Needelman, B. A., I. M. Emmer, S. Emmett-Mattox, S. Crooks, J. P. Megonigal, D. Myers, M. P. J. Oreska, and K. McGlathery. 2018. The Science and Policy of the Verified Carbon Standard Methodology for Tidal Wetland and Seagrass Restoration. *Estuaries and Coasts* 41: 2159–2171.

Neubauer, S. C., K. Givler, S. Valentine, and J. P. Megonigal. 2005. Seasonal Patterns and Plant-Mediated Controls of Subsurface Wetland Biogeochemistry. *Ecology* 86: 3334–3344.

Neubauer, S.C., and J.P. Megonigal. 2015. Moving beyond Global Warming Potentials to Quantify the Climactic Role of Ecosystems. *Ecosystems* 18: 1000-1005.

Nisbet, E. G., M. R. Manning, E. J. Dlugokencky, R. E. Fisher, D. Lowry, S. E. Michel, C. L. Myhre, et al. 2019. Very Strong Atmospheric Methane Growth in the 4 Years 2014–2017: Implications for the Paris Agreement. *Global Biogeochemical Cycles* 33: 318–342.

Nouchi, I., S. Mariko, and K. Aoki. 1990. Mechanism of Methane Transport from the Rhizosphere to the Atmosphere through Rice Plants. *Plant Physiology* 94: 59–66.

Noyce, G. L., M. L. Kirwan, R. L. Rich, and J. P. Megonigal. 2019. Asynchronous nitrogen supply and demand produce nonlinear plant allocation responses to warming and elevated CO2. *Proceedings of the National Academy of Sciences* 116: 21623–21628.

Noyce, G.L., and J.P. Megonigal. 2021. Biogeochemical and plant trait mechanisms drive enhanced methane emissions in response to whole-ecosystem warming. *Biogeosciences* 18: 2449-2463.

Oremland, R. S., and D. G. Capone. 1988. Use of "Specific" Inhibitors in Biogeochemistry and Microbial Ecology. In *Advances in Microbial Ecology*, ed. K. C. Marshall, 285–383. Boston, MA: Springer US.

Oremland, R. S., L. M. Marsh, and S. Polcin. 1982. Methane production and simultaneous sulphate reduction in anoxic, salt marsh sediments. *Nature* 296: 143–145.

Oremland, R. S., and S. Polcin. 1982. Methanogenesis and Sulfate Reduction: Competitive and Noncompetitive Substrates in Estuarine Sediments. *Applied and Environmental Microbiology* 44: 1270–1276.

Oremland, R. S., and B. F. Taylor. 1978. Sulfate reduction and methanogenesis in marine sediments. *Geochimica et Cosmochimica Acta* 42: 209–214.

Parsons, Y. M. and C. M. Lalli. 1984. A Manual of Chemical and Biological Methods for Seawater Analysis. *Geological Magazine* 122: 570–570.

Pastore, M. A., J. P. Megonigal, and J. A. Langley. 2017. Elevated CO2 and nitrogen addition accelerate net carbon gain in a brackish marsh. *Biogeochemistry* 133: 73–87.

Poffenbarger, H. J., B. A. Needelman, and J. P. Megonigal. 2011. Salinity Influence on Methane Emissions from Tidal Marshes. *Wetlands* 31: 831–842.

R Core Team. 2022. R: A Language and Environment for Statistical Computing. RFoundation for Statistical Computing, Vienna,Austria. https://www.R-project.org/.

Reeburgh, W. S. 1969. Observations of Gases in Chesapeake Bay Sediments1. *Limnology and Oceanography* 14: 368–375.

Rosentreter, J. A., A. N. Al-Haj, R. W. Fulweiler, and P. Williamson. 2021. Methane and Nitrous Oxide Emissions Complicate Coastal Blue Carbon Assessments. *Global Biogeochemical Cycles* 35.

Rosentreter, J. A., A. V. Borges, B. R. Deemer, M. A. Holgerson, S. Liu, C. Song, J. Melack, et al. 2021. Half of global methane emissions come from highly variable aquatic ecosystem sources. *Nature Geoscience* 14: 225–230.

Schimel, J. 1995. Plant transport and methane production as controls on methane flux from Arctic wet meadow tundra. *Biogeochemistry* 28: 183–200.

Schink, B., and J. G. Zeikus. 1980. Microbial methanol formation: A major end product of pectin metabolism. *Current Microbiology* 4: 387–389.

Schipper, L. A., and K. R. Reddy. 1994. Methane Production and Emissions from Four Reclaimed and Pristine Wetlands of Southeastern United States. *Soil Science Society of America Journal* 58: 1270–1275.

Schütz, H., W. Seiler, and R. Conrad. 1989. Processes involved in formation and emission of methane in rice paddies. *Biogeochemistry* 7: 33–53.

Scranton, M. I. 1977. The marine geochemistry of methane. Doctoral Dissertation, Massachusetts Institute of Technology and Woods Hole Oceanographic Institution.

Seyfferth, A. L., F. Bothfeld, R. Vargas, J. W. Stuckey, J. Wang, K. Kearns, H. A. Michael, J. Guimond, X. Yu, and D. L. Sparks. 2020. Spatial and temporal heterogeneity of geochemical controls on carbon cycling in a tidal salt marsh. *Geochimica et Cosmochimica Acta* 282: 1–18.

Staver, L., Stevenson, J., Cornwell, J., Nidzieko, N., Staver, K., Owens, M., Logan, L., Kim, C. & Malkin, S. 2020. Tidal marsh restoration at Poplar Island: II. Elevation trends, vegetation development, and carbon dynamics. *Wetlands* 40**,** 1687-1701.

Staver, L. W., Cornwell, J. C., Nidzieko, N. J., Staver, K. W., Stevenson, J. C., Owens, M., Boynton, W. & Lopez-Gonzalez, L. 2021. The Fate of Nitrogen in Dredged Material Used for Tidal Marsh Restoration. *Journal of Marine Science and Engineering* 9.

Stribling, J. M., and J. C. Cornwell. 1997. Identification of important primary producers in a Chesapeake Bay tidal creek system using stable isotopes of carbon and sulfur. *Estuaries* 20: 77–85.

Stribling, J. M., J. C. Cornwell, and O. A. Glahn. 2007. Microtopography in Tidal Marshes: Ecosystem Engineering by Vegetation? *Estuaries and Coasts* 30: 1007–1015.

Tollefson, J. 2022. Scientists raise alarm over “dangerously fast” growth in atmospheric methane. *Nature.* https://doi.org/10.1038/d41586-022-00312-2. Accessed 08 February 2022.

Turner, A. J., C. Frankenberg, and E. A. Kort. 2019. Interpreting contemporary trends in atmospheric methane. *Proceedings of the National Academy of Sciences* 116: 2805–2813.

US Army Corps of Engineers. 2005. General Reevaluation Report. https://www.nab.usace.army.mil/Portals/63/docs/Environmental/PoplarIsland/Poplar%20Island%20GRR%20SEIS.pdf?ver=2016-09-01-093606-857. Accessed 08 August 2022.

US Department of Commerce, National Oceanic and Atmospheric Admistration. 2022. Chesapeake Bay Sentinel Site Cooperative. https://oceanservice.noaa.gov/sentinelsites/chesapeake-bay/. Accessed 30 August 2022.

Valiela, I., J. M. Teal, and N. Y. Persson. 1976. Production and dynamics of experimentally enriched salt marsh vegetation: Belowground biomass1. *Limnology and Oceanography* 21: 245–252.

Wang, C., C. Tong, L. G. Chambers, and X. Liu. 2017. Identifying the Salinity Thresholds that Impact Greenhouse Gas Production in Subtropical Tidal Freshwater Marsh Soils. *Wetlands* 37: 559–571.

Wang, Z., D. Zeng, and W. H. Patrick. 1996. Methane emissions from natural wetlands. *Environmental Monitoring and Assessment* 42: 143–161.

Weston, N. B., R. E. Dixon, and S. B. Joye. 2006. Ramifications of increased salinity in tidal freshwater sediments: Geochemistry and microbial pathways of organic matter mineralization. *Journal of Geophysical Research: Biogeosciences* 111.

Weston, N. B., S. C. Neubauer, D. J. Velinsky, and M. A. Vile. 2014. Net ecosystem carbon exchange and the greenhouse gas balance of tidal marshes along an estuarine salinity gradient. *Biogeochemistry* 120: 163–189.

Weston, N. B., M. A. Vile, S. C. Neubauer, and D. J. Velinsky. 2011. Accelerated microbial organic matter mineralization following salt-water intrusion into tidal freshwater marsh soils. *Biogeochemistry* 102: 135–151.

Whalen, S. C. 2005. Biogeochemistry of Methane Exchange between Natural Wetlands and the Atmosphere. *Environmental Engineering Science* 22:73–94.

Whiticar, M. J. 1999. Carbon and hydrogen isotope systematics of bacterial formation and oxidation of methane. *Chemical Geology* 161: 291–314.

Whiting, G. J., and J. P. Chanton. 1993. Primary production control of methane emission from wetlands. *Nature* 364: 794–795.

Wilson, B. J., B. Mortazavi, and R. P. Kiene. 2015. Spatial and temporal variability in carbon dioxide and methane exchange at three coastal marshes along a salinity gradient in a northern Gulf of Mexico estuary. *Biogeochemistry* 123: 329–347.

Yuan, J., W. Ding, D. Liu, H. Kang, J. Xiang, and Y. Lin. 2016. Shifts in methanogen community structure and function across a coastal marsh transect: effects of exotic Spartina alterniflora invasion. *Scientific Reports* 6.

Zhuang, G.-C., V. B. Heuer, C. S. Lazar, T. Goldhammer, J. Wendt, V. A. Samarkin, M. Elvert, A. P. Teske, S. B. Joye, and K.-U. Hinrichs. 2018. Relative importance of methylotrophic methanogenesis in sediments of the Western Mediterranean Sea. *Geochimica et Cosmochimica Acta* 224: 171–186.

Zelenke, J.L. and J.C. Cornwell. 1996. Sediment accretion and composition in four marshes of Chesapeake Bay. Final Report, Horn Point Environmental Laboratory, Cambridge, MD.